Aus der Klinik für Anästhesiologie m. S. operative Intensivmedizin

der Medizinischen Fakultät Charité – Universitätsmedizin Berlin

DISSERTATION

The role of neuronal steroid receptors and endogenous ligands in pain modulation

zur Erlangung des akademischen Grades

Doctor rerum medicinae

(Dr. rer. medic.)

vorgelegt der Medizinischen Fakultät Charité – Universitätsmedizin Berlin

von

Doaa Mohamed Abdelrahman Mohamed

aus Assuan/Ägypten

Datum der Promotion: 26 / 06 / 2022

Table of contents

List of abbreviations…… i

1. Abstracts…… 1

1.1. English…… 1

1.2. German…… 2

2. Introduction…… 3

2.1. Aldosterone-mineralocorticoid receptors system…… 3

2.2. Aldosterone and MR in the central and peripheral nervous system…… 4

2.3. Modulation of pain by the aldosterone-MR system…… 4

2.4. Aims of PH.D. thesis…… 5

3. Material and methods…… 6

3.1. Animals…… 6

3.2. Intrathecal catheter and osmotic minipump implantation…… 6

3.3. Experimental protocols…… 7

3.4. Western blot…… 7

3.5. Immunohistochemistry…… 8

3.5.1. Tissue preparation …… 8

3.5.2. Double immunofluorescence staining…… 9

3.6. Statistical analysis…… 10

4. Results…… 10

4.1. Co-localization of MR and its protecting enzyme 11ß-HSD2 in sensory dorsal root ganglia…… 10

4.2. Co-localization of aldosterone with both CGRP and MR in sensory dorsal root ganglia…… 13

4.3. Co-localization of aldosterone synthase CYP11B2 with both aldosterone and MR in sensory DRG…… 16

4.4. Reduction of aldosterone-ir neurons and mechanical hyperalgesia following the inhibition of endogenous aldosterone synthase CYP11B2 expressed in dorsal root ganglia …… 20

5. **Discussion** ……...…….…... 21
6. **References** ……..….. 24
7. **Statutory Declaration** ……..……... 32
8. **Declaration of my own contribution to the top-journal publication for a PhD degree** ……,……..……..... 33
9. **Journal Data Filtered By Selected JCR Year: 2019 Selected Editions: SCIE, SSCI Selected Categories: "ANESTHESIOLOGY" Selected Category Scheme: WoS.....** 34
10. **Manuscript of the publication** ……..... 36
11. **Curriculum vitae** (My curriculum vitae does not appear in the electronic version of my paper for reasons of data protection)……. ……
12. **List of publications**……..…….……..….. 50
13. **Acknowledgements** ……..…… 51

List of abbreviations

11β-HSD1……..…...	11β-hydroxysteroid dehydrogenase type 1
11β-HSD2 …….....	11β-hydroxysteroid dehydrogenase type 2
Aldo…….……....	Aldosterone
ANOVA…….....	Analysis of Variance
BSA……...…….…...	Bovine serum albumin
CGRP…….....	Calcitonin gene-related peptide (Neuropeptide marker for nociceptive neurons)
CYP11A1 ……..…...	Cytochrome P450 11A1 (family 11, subfamily A polypeptide 1) (Cholesterol side-chain cleavage)
CYP11B1……..	Cytochrome P450 11B1 (11β-hydroxylase)
CYP11B2 ……	Cytochrome P450 11B2 (18-hydroxylase, Aldosterone synthase)
CYP21……...	Cytochrome P450 21A2 (Steroid 21-hydroxylase)
P450scc……	Cholesterol side-chain cleavage enzyme
DRG ……..…...	Dorsal root ganglion
FAD286 …….…...	Fadrozole (Aldosterone synthase inhibitor)
FCA …….....	Freund's complete adjuvant
FITC green……..…….....	Fluorescein isothiocyanate (green fluorescent dye)
GR …….…...	Glucocorticoid receptor
GR-ir …….……...	GR-immunoreactive
HSD3B1……...	3β-hydroxysteroid dehydrogenase type 1
HSD3B2 ……...	3β-hydroxysteroid dehydrogenase type 2
i.pl…….....	Intraplantar
i.th. ……...	Intrathecal
MR ……...	Mineralocorticoid receptor
-ir ……...…...	-immunoreactive
mRNA ……...…...	Messenger ribonucleic acid
OCT ……..…...	Optimal cutting temperature
PBS ……...…...	Phosphate-buffered saline

RIPA-Buffer …….….....	Radioimmunoprecipitation assay buffer
RNase ……...	Ribonuclease
RT-PCT……..…...	Real Time-Polymerase Chain Reaction
SDS ……...…...	Sodium dodecyl sulfate
StAR ……..…...	Steroidogenic acute regulatory protein (Transport protein)
Texas red ……..	Red fluorescent dye

1. Abstract

1.1. Abstract (English)

Mineralocorticoid receptors (MR) predominantly expressed in peripheral nociceptive neurons demonstrates an essential role for these neuronal MR in the modulation of pain. Indeed, the blocking of MR activation on peripheral nociceptive neurons attenuates inflammatory pain, suggesting an intrinsic involvement of endogenous aldosterone. However, the direct source of endogenous aldosterone and its key processing enzyme is still lacking. Therefore, the work of my thesis examines the localization of MR with its protecting enzyme 11ß-HSD2 as well as its endogenous ligand aldosterone with its processing enzyme aldosterone synthase (CYP11B2) within nociceptive dorsal root ganglion (DRG) neurons of naive rats as well as of rats with Freund's complete adjuvant (FCA)-induced hind paw inflammation. Similar to the well-established renal mineralocorticoid system, the work of my thesis detected the mRNA and corresponding proteins of MR, 11ß-HSD2 and CYP11B2 in DRG neurons. Consistently, double immunofluorescence confocal microscopy demonstrated that the numbers of neurons co-expressing MR with 11ß-HSD2 as well as aldosterone with CYP11B2 were mostly present in CGRP-immunoreactive (-ir) nociceptive neurons. Moreover, the number of CGRP-ir DRG neurons innervating inflamed hind paws and co-expressing MR with 11ß-HSD2 or aldosterone with CYP11B2 were up-regulated. Importantly, blocking aldosterone synthase activity by intrathecal administration of the aldosterone synthase inhibitor FAD286 reduced the number of aldosterone-ir neurons confirming the neuronal synthesis of aldosterone. Altogether, the results of my thesis provide direct evidence of the synthesis of the MR endogenous ligand aldosterone in peripheral nociceptive neurons through the locally expressed enzyme aldosterone synthase.

1.2. Abstrakt (Deutsch)

Die Expression von Mineralocorticoidrezeptoren (MR) vorwiegend in peripheren nozizeptiven Neuronen unterstreicht die essentielle Rolle dieser neuronalen MR bei der Modulation von Schmerzen. In der Tat führte die Blockade einer Aktivierung von MR auf peripheren nozizeptiven Neuronen zu einer Reduktion entzündlicher Schmerzen, was auf eine intrinsische Beteiligung von endogenem Aldosteron hindeutet. Die direkte Quelle für endogenes Aldosteron und sein verantwortliches Schlüsselenzym ist jedoch bisher unbekannt. Daher untersuchte meine Dissertation die Lokalisierung von MR und 11ß-HSD2 sowie von endogenem Aldosteron und dem synthetisierendem Enzym Aldosteronsynthase (CYP11B2) in sensorischen Spinalganglien von naiven Ratten sowie Ratten mit einer Freund's Complete Adjuvans (FCA)-induzierten Hinterpfotenentzündung. In gleicher Weise wie beim etablierten Mineralocorticoid-System der Niere konnte die Arbeit meiner Dissertation die mRNA und die korrespondierenden Proteine von MR, 11ß-HSD2 und CYP11B2 in Spinalganglien-Neuronen nachweisen. Konsistent zeigte die konfokale Doppelimmunfluoreszenz-mikroskopie, dass MR mit 11ß-HSD2 sowie Aldosteron mit CYP11B2 co-exprimiert und hauptsächlich in CGRP-immunreaktiven (ir) nozizeptiven Neuronen vorhanden waren. Darüber hinaus war die Anzahl der sensorischen CGRP-ir-Spinalganglien-Neurone, welche die entzündete Hinterpfote innervieren und MR mit 11ß-HSD2 oder Aldosteron mit CYP11B2 coexprimieren, hochreguliert. Hervorzuheben ist, dass die Blockierung der Aldosteronsynthase-Aktivität durch intrathekale Gabe des Inhibitors FAD286 die Anzahl der Aldosteron-ir-Neuronen verringerte, was die Annahme einer neuronalen Synthese von Aldosteron bestätigte. Zusammenfassend liefern die Ergebnisse meiner Dissertation den Nachweis für eine lokale Synthese des endogenen MR-Liganden Aldosteron durch das Enzym Aldosterone Synthetase, welches in peripheren nozizeptiven Neuronen exprimiert ist.

2. Introduction

2.1. Aldosterone-mineralocorticoid receptors system

The steroid hormone aldosterone plays a vital role in maintaining the body's blood pressure within a normal range through regulating the electrolyte and fluid balance. This occurs by aldosterone's action on the mineralocorticoid receptors (MR) of the collecting ducts within the kidney to stimulate sodium reabsorption and potassium loss, thus, regulating electrolyte homeostasis (Booth et al., 2002).

Aldosterone is synthesized within the zona glomerulosa of the adrenal gland from cholesterol by the actions of four enzymes. These enzymes include cholesterol side-chain cleavage (CYP11A1), 21-hydroxylase (CYP21), and aldosterone synthase (CYP11B2) from the enzyme family of cytochrome P450 enzymes. The CYP11A1 and CYP11B2 are found on the inner mitochondrial membrane, while the endoplasmic reticulum contains CYP21. The fourth enzyme – type 3β-hydroxysteroid dehydrogenase 2 (HSD3B2) – is a member of the short-chain dehydrogenase family within the endoplasmic reticulum (Capponi, 2004). In the first step, the mitochondrial CYP11A1 transforms cholesterol to pregnenolone. It represents the rate-limiting reaction for all the tissues that synthesize steroids and involves the transportation of cholesterol from the cytoplasm to the outer membrane of the mitochondria, followed by the transfer from the outer to the inner mitochondrial membrane, where CYP11A1 is located (Capponi, 2004). This step is mostly dependent on the expression of the phosphorylation of steroidogenic acute regulatory protein (StAR) (Fleury et al., 2004). The pregnenolone translocates to the endoplasmic reticulum to be converted to progesterone by HSD3B2 and possibly HSD3B1 (type 1 3β-hydroxysteroid dehydrogenase) (Konosu-Fukaya et al., 2015). Progesterone is hydroxylated to deoxycorticosterone by CYP21. Three successive oxidation reactions (11β-and18-hydroxylation, followed by18-oxidation) can convert deoxycorticosterone to aldosterone, exclusively by the involvement of aldosterone synthase CYP11B2 in humans (Monticone et al., 2018).

Aldosterone circulates in the blood stream either free (30-50% of total aldosterone) or bound to albumin or corticosteroid-binding globulin (50-70% of total aldosterone) and it is rapidly inactivated in the liver with a plasma half-life of 15 to 20 minutes (Gardner &

Shoback, 2017). Typical MR endogenous ligand aldosterone-sensitive tissues are the kidney (Groeneweg et al., 2011) and heart (Rossignol et al., 2011).

2.2. Aldosterone and MR in the central and peripheral nervous system

Although MR has been expressed in renal and vascular tissue, recent reports have shown that MR is also expressed in other tissues such as the heart, blood vessels, eyes, adipose tissue, and cells of the immune system (Muñoz-Durango et al., 2015). While first evidence of aldosterone synthesis outside of the adrenal glands was neglected (Lockett & Retallack, 1970), previous studies demonstrated aldosterone synthase (CYP11B2) mRNA in cardiac tissue of rodents by Takeda et al. (1995) and then in the failing human heart by (Mizuno et al., 2001; Yoshimura et al., 2002), suggesting extra-adrenal aldosterone synthesis. It has been reported that in the immune response, the aldosterone promotes an inflammatory state characterized by vascular infiltration of immune cells, reactive oxidative stress and proinflammatory cytokine production in various tissues (Herrada et al., 2011). In human leucocytes, the MR expression has been observed in peripheral blood T and B lymphocytes, monocytes, dendritic cells, macrophage and neutrophils (Grafte-Faure et al., 1999). Furthermore, a beneficial effect of MR antagonism in cardiovascular diseases – evidenced by clinical studies(Rossignol et al., 2011)(Rossignol et al., 2011)(Rossignol et al., 2011) - is most likely due to the prevention of inflammatory damage (Rossignol et al., 2011).

In the brain, it has been shown that MR is expressed in neurons of the hippocampal formation, lateral septum, medial and central amygdala, olfactory nucleus, layer II of the cortex, and brain stem (De Kloet et al., 2000a). Furthermore, extra-adrenal aldosterone synthesis has been demonstrated for specific neurons within the brain, e.g. the hypothalamus and rostral ventral medulla, at which aldosterone appears to contribute to the depolarization of neurons (Colombo et al., 2006; MacKenzie et al., 2012).

2.3. Modulation of pain by the aldosterone-MR system

Recent emerging evidence suggests that aldosterone may also play a role in the peripheral nervous system. Corticosteroids exert an analgesic effect in human disease associated with inflammatory pain (De Oliveira et al., 2011).This may occur through either

genomic pathway-mediated anti-inflammatory and immunomodulatory effects or through non-genomic signaling pathways (Barnes et al., 1993; De Oliveira et al., 2011; Garg et al., 2014; Habib et al., 2010). In an animal model of chronic lumbar DRG compression, intrathecal aldosterone antagonism via spironolactone administration reversed mechanical allodynia two days after surgery (Gu et al., 2011). Similarly, the antiallodynic effect of intrathecal spironolactone four and seven days after surgery concomitant with the inhibition of spinal microglia activation and cytokine production was observed in the same animal model (Sun et al., 2012). Moreover, 500 µg of the MR antagonist eplerenone given to the site of zymosan-induced inflammation of the lumbar-DRG reduced mechanical allodynia 1-13 days after intervention (Dong & Xie, 2012). These effects occurred within days and were most likely due to genomic effects through either a prevention of nuclear MR translocation or an attenuation of DRG satellite cell activation (Dong & Xie, 2012). The work of my research group has recently demonstrated MR on peripheral unmyelinated nociceptive C-fibers, suggesting a vital role for the modulation of nociception (Shaqura, Li, Al-Madol, et al., 2016). Indeed, local application of the MR agonist aldosterone at the peripheral and central nerve terminals of nociceptive neurons immediately reversed the inflammation-induced increased mechanical sensitivity (Shaqura, Li, Al-Madol, et al., 2016). This is in line with findings of another group which has shown that aldosterone dose-dependently increased the number of action potentials elicited in acutely-dissociated DRG (Dong & Xie, 2012; Ye et al., 2014). These effects occurred rapidly and were most likely due to non-genomic effects (Shaqura, Li, Al-Madol, et al., 2016).

2.4. Aims of Ph.D. thesis

Based on these findings the project of my thesis (Mohamed et al., 2020) examined in the Wistar rat model of unilateral FCA hind paw inflammation the following hypotheses:

i) Expression of MR and its protecting enzyme 11ß-HSD2 in nociceptive DRG neurons of Wistar rats

ii) Expression of aldosterone with its processing enzyme aldosterone synthase CYP11B2 in nociceptive DRG neurons of Wistar rats

iii) Up-regulation of the expression of aldosterone and its processing enzyme CYP11B2 as well as MR and its protecting enzyme 11ß-HSD2 in nociceptive DRG neurons innervating FCA-inflamed hindpaws of Wistar rats.

iv) Reduction of aldosterone-ir DRG neurons by intrathecal application of the aldosterone synthase inhibitor FAD286 innervating FCA-inflamed hindpaws with consequences for the nociceptive behavior of Wistar rats.

3. Material and methods

3.1. Animals

After approval by the local animal care committee, I performed my experiments in male Wistar rats (180-250g) (breeding facility Charité-Universitätsmedizin Berlin, Germany) in accordance with the European Directive introducing new animal welfare and care guidelines (2010/63/EU). I induced an unilateral hind paw inflammation by an intraplantar (i.pl.) injection of 0.15 ml Freund's complete adjuvant (FCA), a water-in-oil emulsion with killed mycobacteria (Calbiochem, San Diego, CA), under brief isoflurane anesthesia (1.0-2.5 Vol%, Abbott, Wiesbaden, Germany). Within 6 hours, a local swelling and reddening of the right hindpaw develops which further increased up to 24 h and remained stable until the fourth day after FCA-inoculation ((Rittner et al., 2001), on which I performed all experiments.

3.2. Intrathecal catheter and osmotic Minipump implantation

For continuous intrathecal (i.t.) administration of drugs, animals were implanted with chronic intrathecal catheters,as previously described by Shaqura et al.(Shaqura et al., 2013). Animals were anesthetized with isoflurane in oxygen *via* nose cone. A longitudinal skin incision was made in the lumbar region directly above the spinous processes of the L4–L6 vertebrae. The needle through which the catheter was placed (PE10 tubing attached to PE 60 tubing for attachment to an osmotic pump; Portex Ltd, United Kingdom) was set up and inserted at a 30° angle between the L5 and L6 vertebra. Subsequently, the catheter was carefully advanced upward 1 cm into the intrathecal space while rotating it between the thumb and forefingers. The sign of dura penetration was observed by involuntary movements

of the tail or hind limb. Finally, the correct location of the catheter was verified by 10 µl lidocaine 2%, which caused reversible bilateral hind limb paresis for 10 to 15 min.

3.3. Experimental protocols

In the first set of experiments I examined the expression of MR and its protecting enzyme 11ß-HSD2 by western blot and immunohistochemistry in L3-5 DRG neurons of naïve control rats and rats with unilateral hindpaw inflammation. In the next set of experiments, I examined the expression of aldosterone and its processing enzyme CYP11B2 by western blot and immunohistochemistry in L3-5 DRG neurons of naïve control rats and rats with unilateral hindpaw inflammation. In the next set of experiments, I examined potential colocalizations between MR, aldosterone, CYP11B2 and the nociceptive neuron marker CGRP. Finally, I examined whether continuous intrathecal delivery of the aldosterone synthase inhibitor FAD286 will significantly reduce the increased number of aldosterone expressing DRG neurons in Wistar rats with unilateral FCA-hindpaw inflammation. Rats received the following intrathecal treatments over five days starting one day before FCA-induced hindpaw inflammation. For i.t. FAD286 delivery, Alzet osmotic minipumps (2 ml, rate 5.0 µl/h Alzet Corporation, Cupertino, CA) were filled with 0.9% NaCl with or without FAD286 (100 µg/kg*day) and connected to the i.t. catheter to administer FAD286 or vehicle continuously at 5.0 µl/h.

3.4. Western blot

DRG samples from adult rats were solubilized by homogenization in RIPA buffer and the lysate was centrifuged at 16.000 g for 20 min (Chalecka-Franaszek & Cote, 1996). Subsequently, the protein concentration of the supernatant was measured by using a BCA assay (Pierce, Rockford, IL, USA) according to Mousa et al. (2016) to obtain total cell protein. It is important to determine the total protein concentration of the generated extract for loading a specific amount of protein on the gel for comparisons between samples. Subsequently, 10-20 µg protein was denatured in sodium dodecyl sulfate (SDS) sample buffer (5× loading buffer: 200 mM Tris, pH 6.8, 10% SDS, 20% glycerol, 10% 2-mercaptoethanol and 0.05% bromophenol blue; filled up with RIPA buffer) for 10 min at 80℃. This led to binding of SDS to the protein and formed a negatively-charged micelle

around the protein regardless of inherent charges (Shaqura, Li, Al-Madol, et al., 2016). The glycerol is used to simplify the loading by raising the density of the extract and the dye is added to visualize the sample. Heat is applied on the samples to break the structures of the protein (Mahmood & Yang, 2012). When the negatively-charged extracts were loaded on the 7.5% Mini-PROTEAN TGX Stain-Free Precast Gels (Bio-Rad, Copenhagen, Denmark), the different protein bands were separated. Then, the gel was electrophoretically transferred to a nitrocellulose membrane using the Trans-Blot Turbo Transfer System (Bio-Rad Laboratories GmbH, München, Germany) (Shaqura, Li, Al-Madol, et al., 2016). After blotting, membranes were blocked in 3% BSA for 2 h and incubated with mouse anti-CYP11B2 (Merck Millipore, Darmstadt, Germany; 1:1000 in 3% BSA) or rabbit anti-11β−HSD2 (ST John's Laboratory Ltd., London, UK**;** 1:500 in 3% BSA). After incubation with the secondary antibody (peroxidase-conjugated goat anti-rabbit or anti-mouse, 1:40.000, Jackson ImmunoResearch, West Grove, PA) for 2 h at room temperature, reactive protein bands were digitally visualized using ECL solutions (SuperSignal West Pico, Thermo Scientific) in ChemiDoc MP Imager. Finally, the blots were re-probed with monoclonal mouse anti-beta actin antibody (1:20.000; Sigma-Aldrich) as an internal standard. Experiments were conducted on four animals per group.

The western blot bands specific for CYP11B2 (57 kDa) or 11β−HSD2 (70 kDa) were quantified by Java Image processing and analysis software (ImageJ, open-source image software downloaded from the web; http://rsb.info.nih.gov/ij/, accessed March 9, 2018)(Shaqura, Li, Al-Khrasani, et al., 2016; Shaqura, Li, Al-Madol, et al., 2016). The area and density of pixels within the threshold values representing immunoreactivity were measured, and the integrated density (the product of the area and mean of gray values) was calculated. Integrated immunodensities of controls and treated groups were compared and statistically analyzed (Shaqura et al., 2013).

3.5. Immunohistochemistry

3.5.1. Tissue preparation

Adult rats were deeply anesthetized with isoflurane and trans-cardially perfused with 100 ml warm saline, followed by 300 ml 4% (w/v) paraformaldehyde in 0.16 M phosphate

buffer solution (pH 7.4). After perfusion, L3-L5 DRG were removed and fixed in the same fixatives for 90 min, and then cryoprotected overnight at 4˚C in PBS containing 10% sucrose. The tissues were then embedded in tissue-Teck compound (OCT, Miles Inc. Elkhart, Indiana) and frozen. 8 µm sections were cut by using a Cryostat (Thermo Fisher, Dreieich, Germany) and they were mounted onto gelatin-coated slides (Shaqura, Li, Al-Madol, et al., 2016).

3.5.2. Double immunofluorescence staining

Double immunofluorescence staining was processed as previously described (Mousa et al., 2007; Shaqura, Li, Al-Madol, et al., 2016). Tissue sections were incubated for 60 min in PBS containing 0.3% Triton X-100, 1% BSA, 10% goat serum (Vector Laboratories, CA, USA) (blocking solution) to prevent non-specific binding. Tissue sections were then incubated overnight with the following primary antibodies: polyclonal rabbit anti-aldosterone (Novus Biologicals, LLC, CO, USA, 1:500), in combination with a polyclonal guinea pig anti-CGRP, monoclonal mouse anti-MR (private gift from Prof. Elise Gomez-Sanchez, Jackson, USA) or CYP11B2. In addition, polyclonal sheep antibody against 11β−HSD2 was examined in combination with the monoclonal mouse anti-MR (private gift from Prof. Elise Gomez-Sanchez, Jackson, USA). After incubation with primary antibodies, the tissue sections were washed with PBS and then incubated with Alexa Fluor 594 donkey anti-rabbit antibody (Vector Laboratories) in combination with Alexa Fluor 488 goat anti-guinea pig, anti-mouse or anti-sheep antibody (Invitrogen, Germany). Thereafter, sections were washed with PBS, and the nuclei-stained bright blue with 40-6-Diamidino-2-phenylindole (DAPI) (0.1 mg/ml in PBS) (Sigma). Finally, the tissue sections were washed in PBS, mounted on vectashield (Vector Laboratories) and imaged on a LSM510confocal laser scanning microscope,as previously described (Li et al., 2018) – equipped with an argon laser (458/488/514 nm), a green helium/neon laser (543 nm), and a red helium/neon laser (633 nm; Carl Zeiss, Gottingen, Germany). Single optical slice images were taken using ×10 or ×20 Plan-Neofluar air interface or ×40 Plan-Neoflua oil interface objective lens. The brightness and contrast of the final images were adjusted in Adobe Photoshop 6.0 (Adobe Systems, San Jose, CA). To demonstrate specificity of the staining, the following controls were included as described in the previous work of my lab group (Li et al., 2018; Mousa et

al., 2016; Shaqura, Li, Al-Khrasani, et al., 2016), namely the omission of either the primary antisera or the secondary antibodies.

The method of quantification for DRG staining has been previously described (Al-Madol et al., 2017; Li et al., 2018; Mousa et al., 2016; Shaqura, Li, Al-Khrasani, et al., 2016). In order to count the total number of neurons, only those immuno-stained neurons containing a distinct nucleus were counted from 2-3 sections per rat and 4-5 rats per group using 40x objective lens. In a similar way, the number of aldosterone/total DRG, MR/total DRG, 11β−HSD2 /total DRG, CYP11B2/total DRG, aldosterone+MR/total DRG, CGRP+aldosterone/total DRG, CGRP+CYP11B2/total DRG, CGRP+11β−HSD2/total DRG, aldosterone+CYP11B2/total DRG, CGRP+11β−HSD2 /total DRG were counted in each DRG sections and represented as percentages.

3.6. Statistical analysis

All tests were performed using Sigma Plot 13.0 software (SPSS Inc., Germany). Taqman® PCR, western blot as well as immunofluorescence data were analyzed as two group comparisons (FCA-treated rats versus controls) by the two-tailed independent Student t-test in case of normally-distributed data. Multiple comparisons were analyzed by one-way ANOVA and post-hoc Tukey test. For all statistical tests, significance was assumed at $P<0.05$.

4. Results

4.1. Co-localization of MR and its protecting enzyme 11-ßHSD2 in sensory dorsal root ganglia

Western blot experiments using a specific antibody against11ß-HSD2 identified a protein band at the expected molecular weight of 70 kDa in DRG of control rats and rats with FCA-inflamed hind paws (Fig. 1A). The intensity of these protein bands appeared slightly different, while the ß-actin protein bands (expected molecular weight of 43 kDa) - used as an internal loading control - did not seem different (Fig. 1A). Quantitative analyses of the integrated optical density showed no statistically significant differences between the integrated optical intensities of the 11ß-HSD2 protein bands of controls versus FCA-treated

rats (Fig. 1B). Immunofluorescence staining of DRG from rats with FCA-induced hind paw inflammation and control rats using a specific anti-MR antibody identified MR-immunoreactivity in several DRG neurons with a small-to-medium cell size (Fig. 2A, B). Quantitative analyses of the number of DRG neuronal cells immunoreactive for MR divided by the total number of neuronal cells per image revealed a significant increase of MR-ir cells in DRG innervating inflamed versus control hind paws (Fig.2C). Immunofluorescent staining of DRG from rats with FCA-induced hind paw inflammation and control rats using a specific anti-11ß-HSD2 antibody identified 11ß-HSD2-immunoreactivity in several DRG cells (Fig. 2D, E). Quantitative analyses of the number of DRG cells positive for 11ß-HSD2 divided by the total number of cells per image revealed a significant increase of 11ß-HSD2-positive cells in DRG innervating inflamed versus control hind paws (Fig. 2F). Examining the same sections with fluorescence microscopy by using both a filter for Texas red and FITC green fluorescence demonstrated that 11ß-HSD2 immunoreactivity overlap with MR in DRG cells (Fig. 2G, H). Quantitative analysis of the number of DRG cells immunoreactive for both MR and 11ß-HSD2 divided by the total number of neuronal cells per image revealed a significant increase in the co-localization of 11ß-HSD2 with MR-ir cells in DRG innervating inflamed versus control hind paws (Fig. 2 I).

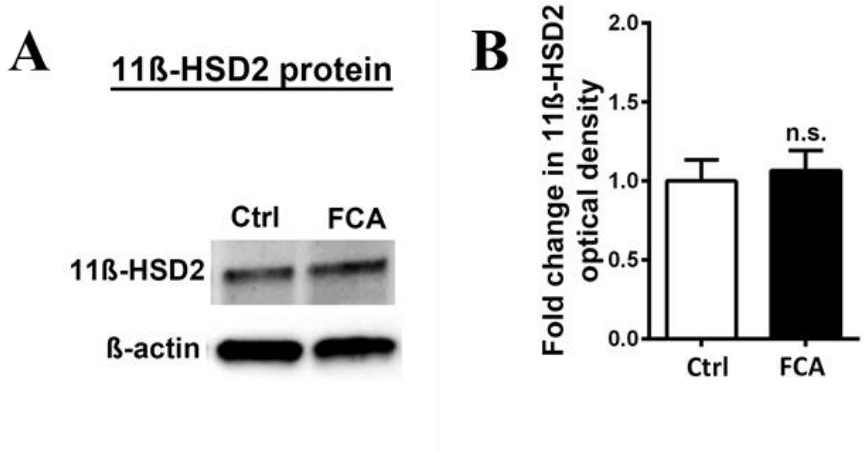

Figure 1: Detection of 11β-hydroxysteroid-dehydrogenase 2 (11ß-HSD2) protein in dorsal root ganglia innervating Freund's Complete Adjuvant (FCA)-inflamed hind paws of rats compared to DRG of control rats (Ctrl) using Western blot. shows a representative western blot with a 11-ßHSD2 protein band (at 70 kDa) and a ß-actin protein band (at 43 kDa) as internal loading control; **(B)** shows fold changes of the integrated optical density of 11ß-HSD2 protein bands by Java Image

processing and analysis software. Note that the differences between the two groups did not significantly differ (n.s.) (n=4-5 rats, P = 0.72, two-tailed independent Student t-test). (This figure was modified from the published figure in Mohamed et al., 2020, Anesthesiology 132(4):867-880).

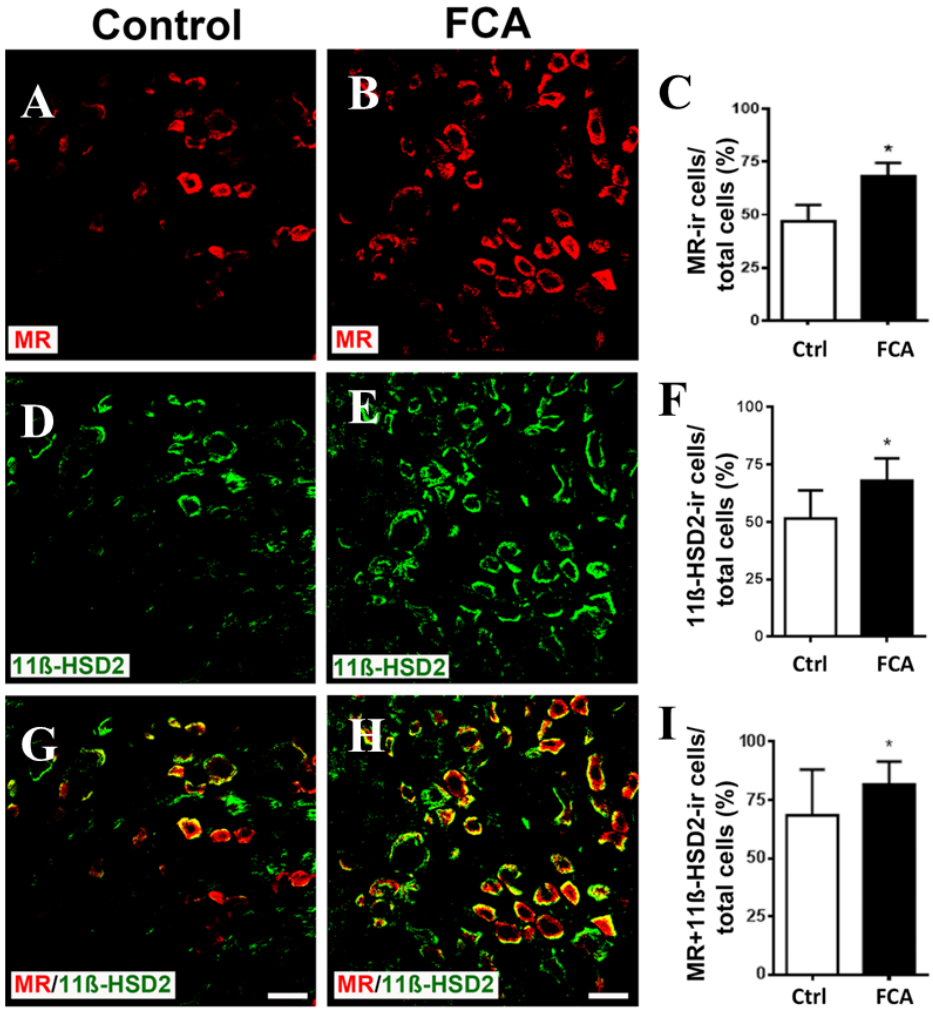

Figure 2: Double immunofluorescence confocal microscopy of 11β-hydroxysteroid-dehydrogenase 2 (11ß-HSD2) co-localized with mineralocorticoid receptors (MR) in dorsal root ganglia (DRG) innervating FCA-inflamed rat hind paws compared to dorsal root ganglia of controls. A and B show a positive immunofluorescence staining for MR (*Texas red fluorescence*) using a monoclonal mouse anti-MR antibody (private gift from Dr. Elise Gomez-Sanchez)**. C** displays the ratio of MR-ir neurons to the total number of neuronal cells in the same image (Ctrl: 47 ± 2%; n=14 images, FCA: 68 ± 1,5%; n=16 images; P<0.05; two-tailed independent Student's). **D and E** show a positive immunofluorescence staining for 11ß-HSD2 (*FITC green fluorescence*) using a polyclonal sheep anti-11ß-HSD2 antibody (Elise Gomez-Sanchez, Jackson, USA)**. F** displays the ratio of 11ß-HSD2-ir neurons to the total number of neuronal cells in the same image (Ctrl: 51 ± 3%; n=14 images, FCA: 68 ± 2, 4; n=16 images, P<0.05; two-tailed independent Student's). **G and H** show the co-localization of 11ß-HSD2 immunoreactivity with MR in DRG neurons. **I** displays the ratio of neurons co-express 11ß-HSD2 with MR to the total number of neuronal cells in the same image (Ctrl: 68 ± 5%; n=14 images, FCA: 81.60 ± 2%; n=16 images, P<0.05; two-tailed independent

Student's). Data are expressed as means ± SD. Bar = 40 μm. (This figure was modified from the figure published in Mohamed et al., 2020, Anesthesiology 132(4):867-880).

4.2. Co-localization of aldosterone with both CGRP and MR in sensory dorsal root ganglia

Double immunofluorescence confocal microscopy using specific antibodies against aldosterone and CGRP showed a co-localization of aldosterone immunoreactivity (Fig. 3A, B) with CGRP in DRG cells (Fig. 3D, E) innervating FCA-inflamed or non-inflamed rat hind paws. Quantitative analyses of these tissue sections from DRG revealed a significant increase in both aldosterone- and CGRP-ir neuronal cells (Fig. 3C, F). Aldosterone- and CGRP-ir double-labelled neuronal cells of DRG were identified using both a filter for Texas red and FITC green fluorescence (Fig. 3G, H). Quantitative analyses of the number of DRG neuronal cells immunoreactive for both aldosterone and CGRP divided by the total number of neuronal cells per image revealed a significant increase in DRG innervating inflamed versus control hind paws (Fig. 3 I). In addition, double immunohistochemistry demonstrated the co-existence of aldosterone (Texas red fluorescence) with MR (FITC green fluorescence) in DRG neurons (Fig. 4 A, B and D, E). Quantitative analysis of the ratio of aldosterone- as well as MR-ir DRG neuronal cells in relation to the total number of cells per image showed a significant increase of aldosterone- as well as MR-ir DRG cells in FCA-treated rats compared to controls (Fig. 4C, F). Examining the same sections by using both a filter for Texas red and FITC green fluorescence revealed a co-localization of aldosterone with MR (Fig. 4I). The proportion of DRG cells co-expressing aldosterone immunoreactivity with MR was significantly increased in relation to the total number of neuronal cells per image following FCA hind paw inflammation compared to the control (Fig. 4 I).

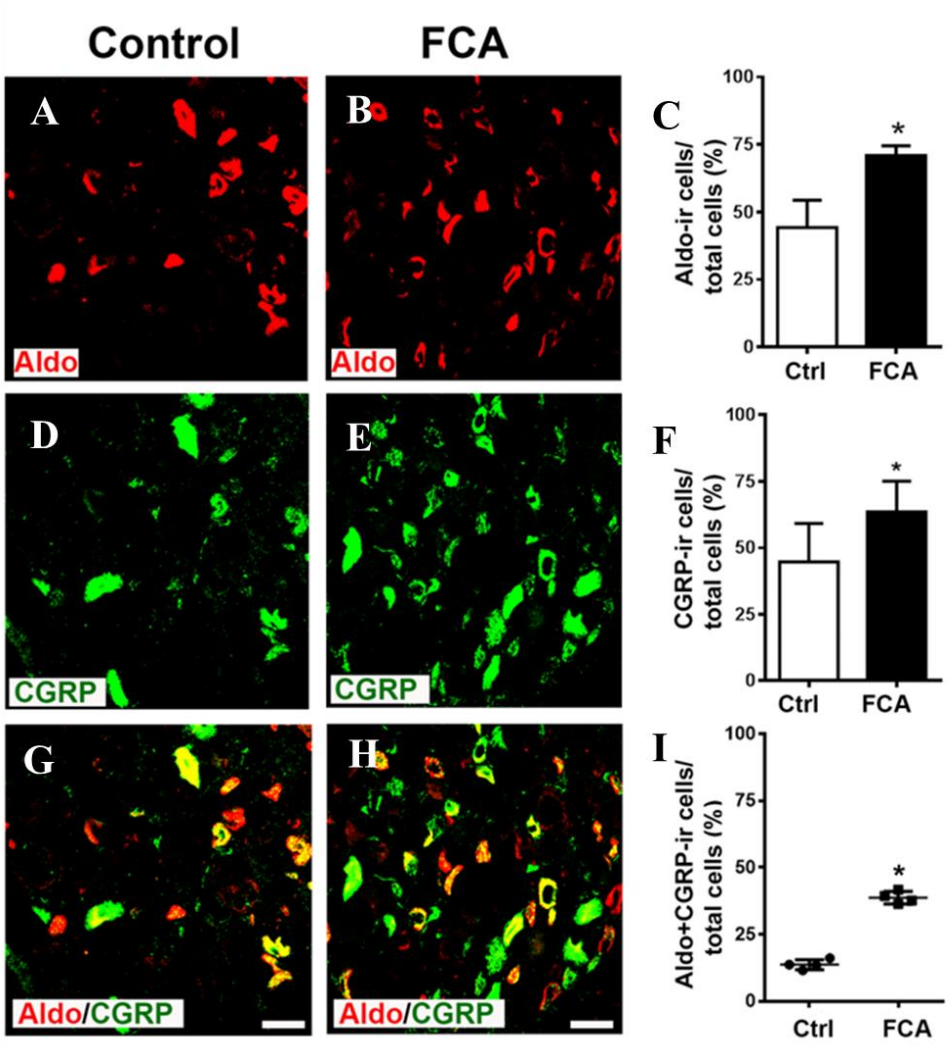

Figure 3: Double immunofluorescence confocal microscopy of aldosterone (Aldo) co-localized with the sensory neuron marker calcitonin gene-related peptide (CGRP) in DRG innervating rats with FCA-inflamed hind paws compared to that of controls. A and B show a positive immunofluorescence staining for aldosterone *(Texas red fluorescence*) using polyclonal rabbit anti-aldosterone antibody (Novus Biologicals, LLC, CO, USA). **C** displays the ratio of aldosterone-ir neurons to the total number of neuronal cells in the same image (Ctrl: 45 ± 3%; n=20 images, FCA: 66 ± 2 %; n=20 images, P<0.05; two-tailed independent Student's). **D and E** show a positive immunofluorescence staining for CGRP *(FITC green fluorescence)* using polyclonal guinea pig anti– CGRP (Peninsula Laboratories, CA, USA). **F** displays the ratio of CGRP-ir neurons to the total number of neuronal cells in the same image (Ctrl: 44 ± 1%; n=7 images, FCA: 66 ± 4 %; n=8 images, P<0.05; two-tailed independent Student's). **G and H** show the co-localization of aldosterone immunoreactivity in CGRP-ir DRG neuronal cells of inflamed hind paws versus controls. **I** displays the ratio of neurons co-expressing aldosterone with CGRP to the total number of neuronal cells in the same image (Ctrl: 14 ± 1%; n=7 images, FCA: 39 ±1 %; n=8 images, P<0.05; two-tailed independent Student's). Data are expressed as means ± SD. Bar = 40 µm. (This figure was modified from the figure published in Mohamed et al., 2020, Anesthesiology 132(4):867-880).

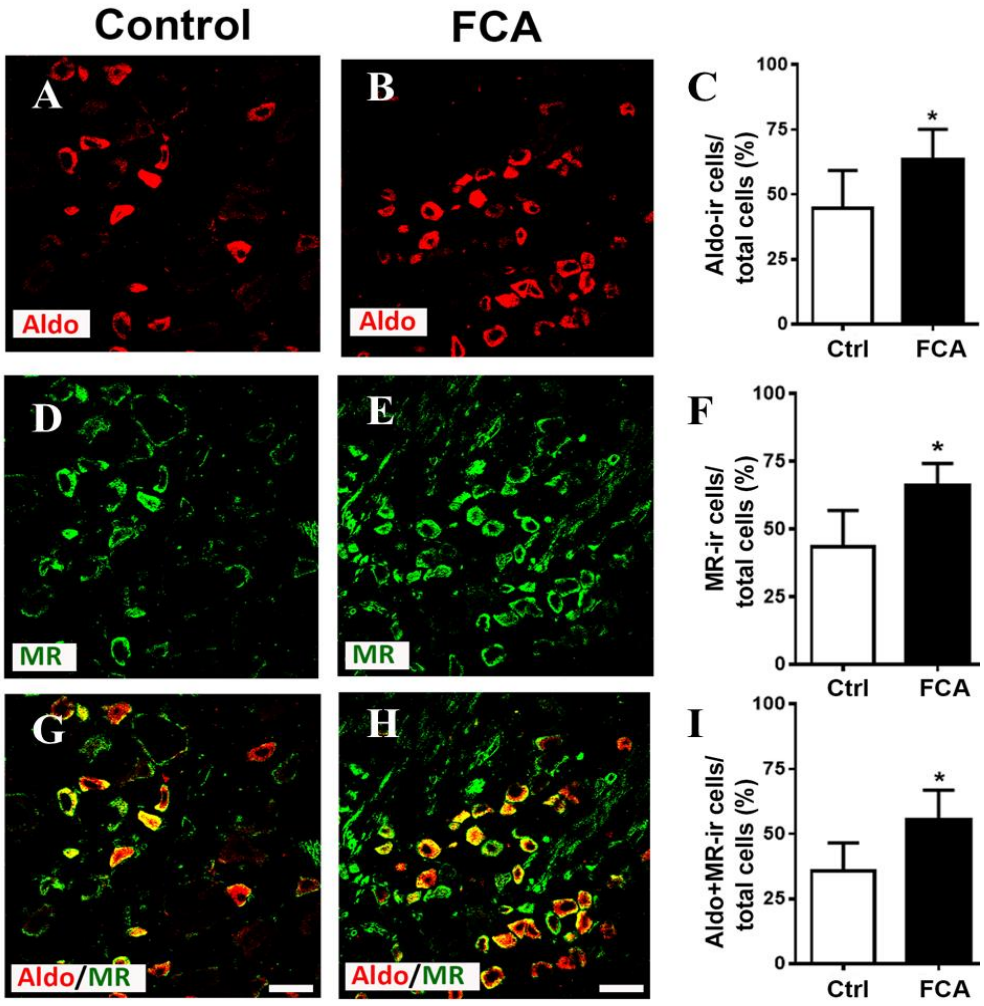

Figure 4: Double immunofluorescence confocal microscopy of aldosterone (Aldo) with the **mineralocorticoid receptor (MR) in dorsal root ganglia (DRG) innervating FCA-inflamed rat hind paws compared to that of controls. A and B** show a positive immunofluorescence staining for aldosterone (*Texas red fluorescence*) using polyclonal rabbit anti-aldosterone (Novus Biologicals, LLC, CO, USA)**. C** displays the ratio of aldosterone-ir neurons to the total number of neuronal cells in the same image (Ctrl: 45 ± 4%; n=14 images, FCA: 64 ± 3%; n=13 images, P<0.05; two-tailed independent Student's). **D and E** show a positive immunofluorescence staining for MR (*FITC green fluorescence*) using a monoclonal mouse anti-MR antibody (private gift from Dr. Elise Gomez-Sanchez)**. F** displays the ratio of MR-ir neurons to the total number of neuronal cells in the same image (Ctrl: 44 ± 4%; n=14 images, FCA: 66 ± 2%; n=13 images, P<0.05; two-tailed independent Student's). **G and H** show the co-localization of aldosterone with MR in DRG of inflamed hind paws versus controls. **I** displays the ratio of DRG neurons co-express aldosterone with MR to the total number of neuronal cells in the same image (Ctrl: 36 ± 3 %; n=14 images, FCA: 55 ± 3%; n=13 images, P<0.05; two-tailed independent Student's). Data are expressed as means ± SD. Bar = 40 µm. (This figure was modified from the figure published in Mohamed et al., 2020, Anesthesiology 132(4):867-880).

4.3. Co-localization of aldosterone synthase CYP11B2 with both aldosterone and MR in sensory DRG

Western blot experiments identified CYP11B2 specific protein bands (57 kDa) in sensory DRG cells by using a specific anti-CYP11B2 antibody. Quantitative analysis of the integrated optical density of CYP11B2 specific protein band in using J-image showed no statistically significant difference between the integrated optical intensities of the CYP11B2 protein bands in DRG of FCA-treated rats compared to that of controls (Fig. 5B).

Immunofluorescence staining of DRG using a specific anti-aldosterone and anti-CYP11B2 antibody demonstrated aldosterone and CYP11B2 immunoreactivity within DRG neurons of rats with FCA-induced hind paw inflammation and controls (Fig. 6 A, B and D, E). Quantitative analysis of the ratio of aldosterone- as well as CYP11B2-ir DRG neuronal cells in relation to the total number of cells per image showed a significant increase of aldosterone as well as CYP11B2–ir DRG cells in FCA-treated rats compared to controls (Fig. 6C, F). Examining the same sections by using a filter for both Texas red and FITC green fluorescence revealed a co-localization of aldosterone with CYP11B2 (Fig. 6G, H). Quantitative analyses of the double-labeled DRG cells showed a significant increase of the number of neuronal cells that co-express CYP11B2 with aldosterone in DRG innervating inflamed hind paws versus that of the control (Fig. 6 I).

Furthermore, MR- and CYP11B2-ir DRG neurons increased in the DRG of FCA-treated rats versus controls (Fig. 7 A, B) (Fig. 7 D, E). Quantitative analyses of the number of DRG neuronal cells immunoreactive for MR divided by the total number of neuronal cells per image revealed a significant increase of MR-ir DRG neuronal cells. In addition, the number of DRG neuronal cells immunoreactive for CYP11B2 divided by the total number of cells per image revealed a significant increase of CYP11B2 -ir DRG neuronal cells of DRG innervating inflamed versus control hind paws (Fig. 7C, F). Examining the same sections with fluorescence microscopy by using both filters (for Texas red and FITC green fluorescence), they demonstrate abundant overlap of MR with CYP11B2 immunoreactivity (Fig. 7G, H). Quantitative analyses of the number of DRG neuronal cells immunoreactive for MR with CYP11B2 divided by the total number of neuronal cells per image revealed a

significant increase of co-localization of CYP11B2 with MR in DRG innervating inflamed versus control hind paws (Fig. 7 I).

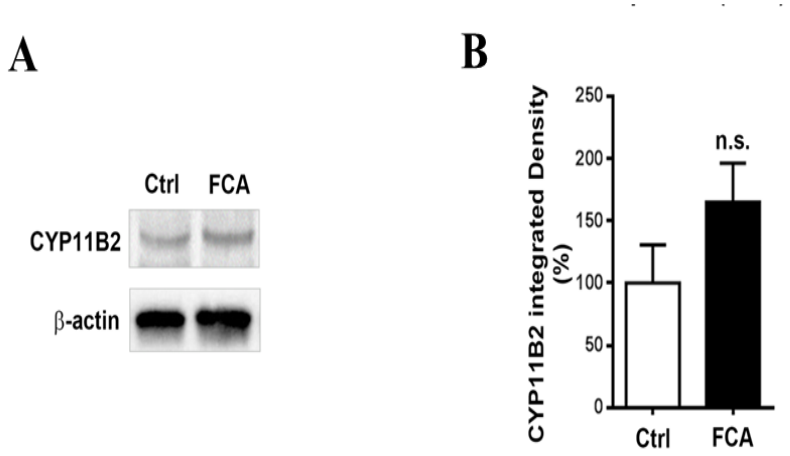

Figure 5: Detection of aldosterone synthase enzyme CYP11B2 using Western blot in dorsal root ganglia innervating FCA-inflamed rat hind paws compared to controls (Ctrl) without any inflammation. A shows a representative western blot with a CYP11B2-specific protein band at the expected molecular weight of 57kDa detected by anti-CYP11B2 antibody (Merck Millipore, Germany) and a ß-actin protein band (43kDa, anti-ß-actin antibody, Sigma-Aldrich) for internal loading control. **B** shows the quantitative analysis of the integrated optical density of the respective protein bands of CYP11B2 by J-Image software (software downloaded from: http://rsb.info.nih.gov/ij/, accessed March 9, 2018) without any significant difference between groups (non-significant; n.s), P = 0.189, two-tailed independent Student t-test). (This figure was modified from the figure published in Mohamed, et al.; Anesthesiology 2020; 132 (4):867-880).

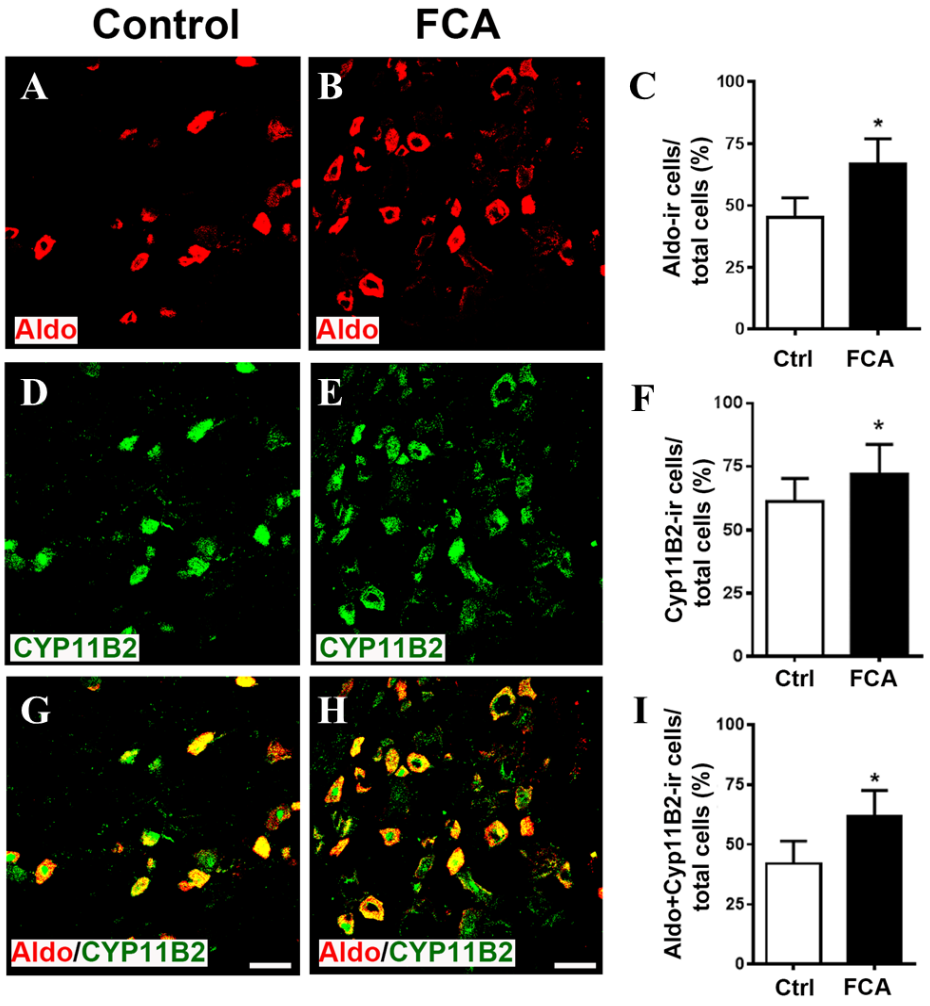

Figure 6: Double immunofluorescence confocal microscopy of aldosterone (Aldo) co-localized with aldosterone synthase enzyme CYP11B2 in dorsal root ganglia innervating FCA-inflamed rat hind paws compared to that of controls. A and B show a positive immunofluorescence staining for aldosterone (*Texas red fluorescence*) using polyclonal rabbit anti-aldosterone antibody (Novus Biologicals, LLC, CO, USA). **C** displays the ratio of aldosterone-ir neurons to the total number of cells in the same image (Ctrl: 45 ± 2 %; n=15 images, FCA: 67 ± 3%; n=12 images, P<0.05; two-tailed independent Student's). **D and E** show a positive immunofluorescence staining for CYP11B2 (*FITC green fluorescence*) using monoclonal mouse anti– CYP11B2 antibody (Millipore; Darmstadt, Germany). **F** displays the ratio of CYP11B2-ir neurons to the total number of neuronal cells in the same image (Ctrl: 61 ± 2%; n=15 images, FCA: 72 ± 4%; n=12 images, P<0.05; two-tailed independent Student's). **G and H** show the co-localization of aldosterone with CYP11B2 in DRG of inflamed hind paws versus controls. **I** displays the ratio of neurons co-express aldosterone with CYP11B2 to the total number of neuronal cells in the same image (Ctrl: 38 ± 2%; n=8 images, FCA: 60 ± 2 %; n=9 images, P<0.05; two-tailed independent Student's). Data are expressed as means ± SD. Bar = 40 µm. (This figure was modified from the figure published in Mohamed, et al.; Anesthesiology 2020; 132(4):867-880).

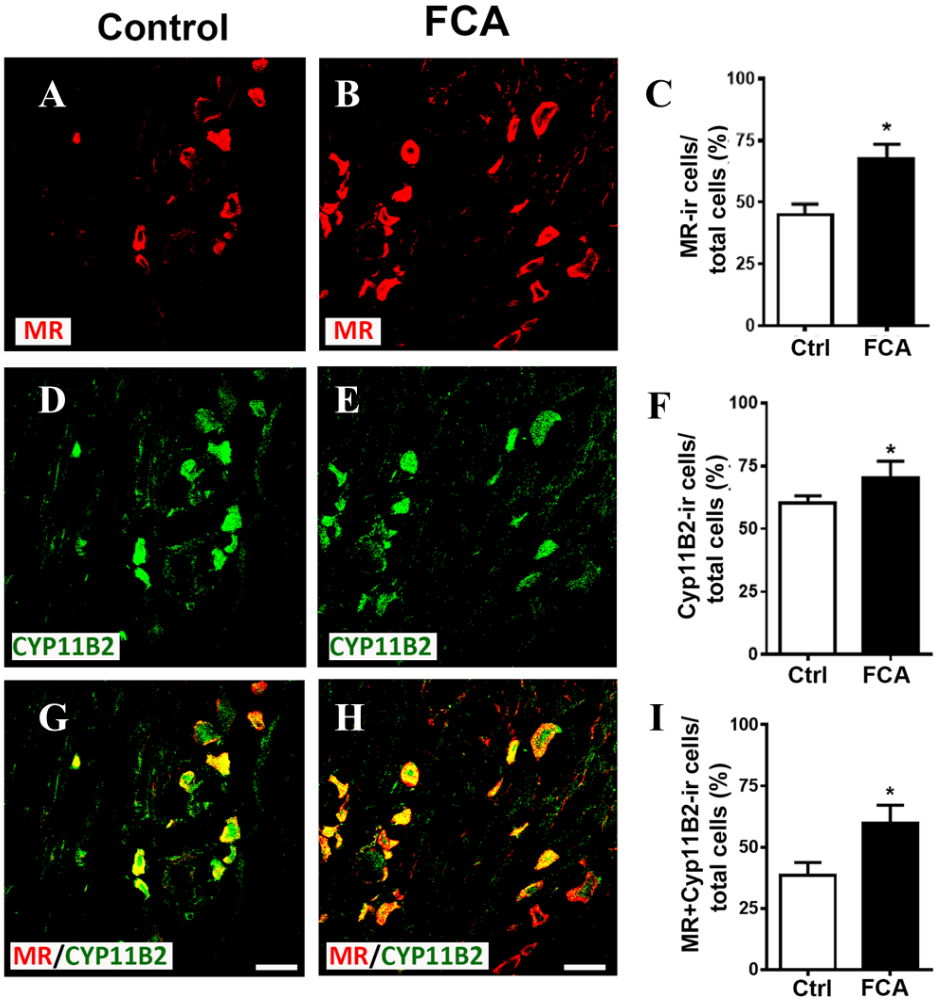

Figure 7: Double immunofluorescence confocal microscopy mineralocorticoid receptors (MR) co-localized with Aldosterone Synthase (CYP11B2) in dorsal root ganglia innervating FCA-inflamed rat hind paws compared to that of controls. A and B show positive immunofluorescence staining for MR (*Texas red fluorescence*) using a monoclonal mouse anti-MR antibody (private gift from Dr. Elise Gomez-Sanchez)**. C** displays the ratio of MR-ir neurons to the total number of neuronal cells in the same image (Ctrl: 45 ± 2%; n=7 images, FCA: 67 ± 2 %; n=8 images, P<0.05; two-tailed independent Student's). **D and E** show a positive immunofluorescence staining for CYP11B2 (*FITC green fluorescence*) using monoclonal mouse anti-CYP11B2 (Millipore; Darmstadt, Germany)**. F** displays the ratio of CYP11B2 -ir neurons to the total number of neuronal cells in the same image (Ctrl: 60 ± 1%; n=7 images, FCA: 70 ± 3%; n=8 images, P<0.05; two-tailed independent Student's). **G and H** show the co-localization of CYP11B2 with MR in DRG neurons. **I** displays the ratio of neurons colocalizing CYP11B2 with MR to the total number of neuronal cells in the same image (Ctrl: 38 ± 2%; n=8 images, FCA: 59 ± 2%; n=9 images, P<0.05; two-tailed independent Student's). Data are expressed as means ± SD. Bar = 40 µm. (This figure was modified from the figure published in Mohamed, et al.; Anesthesiology 2020; 132(4):867-880).

4.4. Reduction of aldosterone-ir neurons and mechanical hyperalgesia following the inhibition of endogenous aldosterone synthase CYP11B2 expressed in dorsal root ganglia

Immunohistochemistry of aldosterone in DRG showed that the FCA-inflammation-induced increase in the number of aldosterone-ir neuronal cells was reversed by chronic intrathecal treatment with the aldosterone synthase inhibitor FAD286 (Fig. 8A-C). Quantitative analyses of aldosterone-ir neuronal cells in tissue sections of DRG revealed that the ratio of aldosterone positive neuronal cells to the total number of DRG neurons significantly increased following FCA-induce hind paws inflammation compared to controls, which was significantly abolished following chronic intrathecal treatment with the aldosterone synthase inhibitor FAD286 (Fig. 8 D).

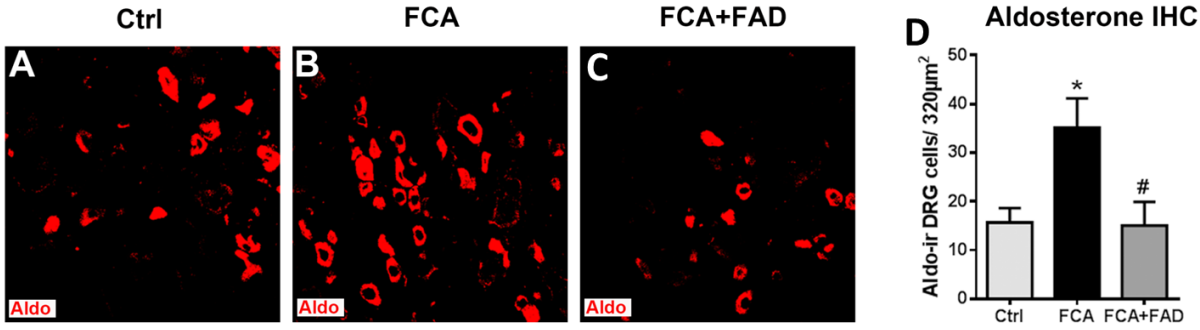

Figure 8: Effect of aldosterone synthase inhibitor FAD286 on the expression of aldosterone in dorsal root ganglia (DRG) innervating FCA-inflamed rat hind paws compared to that of control rats. A-C show a positive immunofluorescence of aldosterone (*Texas red fluorescence*) using a polyclonal rabbit anti-aldosterone antibody (Novus Biologicals, LLC, CO, USA) in DRG of rats with FCA hind paw inflammation and rats with FCA hind paw inflammation treated with intrathecal FAD286 over four days compared to control rats without any inflammation. **D** displays the ratio of aldosterone-ir neurons to the total number of neuronal cells (Ctrl: 16 ± 1%; n=6 images, FCA: 35 ± 2%; n=7 images, FCA+FAD: 15 ± 1%; n=11 images). **P<0.0001* significant difference between DRG of controls (Ctrl) and FCA-inflamed rats; #P<0.0001 significant difference between FCA-inflamed rats and FCA-inflamed rats treated with synthase inhibitor FAD286 (one-way repeated measurement ANOVA, followed by post-hoc Dunnett test). (This figure was modified from the figure published in Mohamed, et al.; Anesthesiology 2020; 132(4):867-880).

5. Discussion

The results of my thesis show that: (1) MR proteins are identified in peripheral DRG neurons by western blot and immunohistochemistry; (2) in these neurons, MR – similar to their presence in kidney tissue – colocalize with 11ß-HSD2, an enzyme that prevents MR activation by corticosterone through its fast degradation; (3) the co-localization of MR with 11ß-HSD2 in sensory DRG neurons innervating FCA-inflamed hind paws is up-regulated; (4) the endogenous ligand aldosterone for MR is detected in nociceptive CGRP-ir DRG neurons and co-localizes with MR suggesting a presumable paracrine action; (5) the enzyme aldosterone synthase (CYP11B2) – which catalyzes the final conversion of 18OH-corticosterone into aldosterone – is demonstrated in aldosterone-ir DRG neurons; and (6) the inhibition of the enzyme aldosterone synthase by intrathecal application of FAD286 results in a significant reduction in the number of aldosterone-ir neurons.

It is well established that MR is expressed in kidney tissue (Manders et al., 1993) and other peripheral tissues (Slight et al., 1996). MR has recently been demonstrated in neurons of the hippocampal formation, lateral septum, medial and central amygdala, olfactory nucleus, layer II of the cortex, and brain stem sensory and motor neurons (De Kloet et al., 2000b). Indeed, MR and GR were detected in hippocampal neurons using mouse monoclonal antibody against the GR and rabbit antiserum against the MR by double-labeling immunocytochemistry (van Steensel et al., 1996). In previous work of my lab group MR were identified in sensory neurons of DRG and dorsal horn of spinal cord using immunofluorescence confocal microscopy (Shaqura et al., 2016). In agreement with these findings, MR immunoreactivity was identified in presynaptic terminals and postsynaptic densities of synaptic areas of the central nervous system by electron microscopy (Prager et al., 2010; Johnson et al., 2005).

MR can not only be stimulated by aldosterone but also by corticosterone (Elise Gomez-Sanchez & Celso E. Gomez-Sanchez, 2014). However, MR protecting enzyme 11ß-HSD2 prevents MR stimulation by corticosterone through converting the biologically-active corticosterone to the inactive 11-dehydrocorticosterone, which allows MR activation exclusively by aldosterone (Chapman et al., 2013). Interestingly, I was able to identify 11ß-

HSD2 protein in DRG neurons by western blot. Moreover, double immunofluorescence confocal microscopy confirmed that 11ß-HSD2 predominantly co-localized with MR immunoreactivity within peripheral DRG neurons (Ctrl: 68 ± 5%, FCA: 81.60 ± 2%) (Mohamed et al., 2020). In agreement with the present finding, several studies have shown the presence of MR and 11ß-HSD2 in non-epithelial tissues, such as the heart (Lombès et al., 1995) and brain (Zhang et al., 2006). Moreover, my results are consistent with previous work of my group demonstrating that 11ß-HSD2 co-localized with a neuronal marker CGRP for peptidergic sensory neurons in DRG (Li et al., 2018). Additionally, 11ß-HSD2 protein and mRNA are expressed with MR in the paraventricular nucleus and supraoptic nuclei of the hypothalamus, suggesting that MR in the brain are mostly controlled by aldosterone (Haque et al., 2015; Zhang et al., 2006).

It is well established that aldosterone is synthesized within the adrenal gland and its physiological effects are elicited by binding to the nuclear MR in the epithelial cells of the kidney (Manders et al., 1993). However, recent emerging evidence indicates that the corticosteroids including aldosterone also have an extra-adrenal site of synthesis and show local paracrine effects. Consistently, a previous study detected the key gene P450scc involved in aldosterone biosynthesis through converting cholesterol to pregnenolone in glial cells using immunohistochemistry (Testas et al., 1989). Moreover, P450scc has been demonstrated in neurons such as fetal rat primary hippocampal cells and Purkinje cells of the rat cerebellum (Furukawa et al., 1998). Moreover, the key gene StAR protein involved in aldosterone biosynthesis – which stimulates steroid biosynthesis by increasing the transfer of cholesterol to the inner mitochondrial matrix – has been detected in the brain areas(Connell & Davies, 2005; Furukawa et al., 1998). In my experiments, I demonstrated abundant aldosterone immunoreactivity in peripheral CGRP positive nociceptive neurons using double immunofluorescence confocal microscopy. Moreover, the aldosterone immunoreactivity was predominantly co-localized with MR in DRG peripheral sensory neurons (Mohamed et al., 2020). The present findings confirm the previous reports suggesting extra-adrenal aldosterone synthesis, e.g. within the paraventricular nucleus of the hypothalamus and the forebrain circumventricular organs as well as the subfornical organ (Colombo et al., 2006; Elise Gomez-Sanchez & Celso E. Gomez-Sanchez, 2014; Wang et al., 2016). Importantly, in my experiments the number of aldosterone immunoreactive DRG neurons co-localizing

with CGRP or with MR was significantly increased following four days of painful FCA-induced hindpaw inflammation (Mohamed et al., 2020) suggesting the important role of endogenous aldosterone to modulate the inflammatory process.

Aldosterone synthase CYP11B2 is a cytochrome P450 enzyme located on the inner mitochondrial membrane and encoded by CYP11B2 gene. Aldosterone synthase is responsible for synthesis of aldosterone by three consecutive reactions through converting (1) 11-deoxycorticosterone to corticosterone, (2) corticosterone to 18-hydroxycorticosterone, (3) and finally 18-hydroxycorticosterone to active aldosterone (Connell & Davies, 2005). In order to further support the local aldosterone production within peripheral sensory DRG neurons, I investigated the existence of processing enzyme aldosterone synthase CYP11B2 within peripheral sensory neurons. Indeed, I successfully identified the aldosterone synthase CYP11B2 protein band in peripheral sensory DRG neurons using western blot technique. Moreover, I demonstrated the co-localization of aldosterone synthase CYP11B2 with aldosterone as well as MR immunoreactivity within peripheral sensory DRG neurons using double immunofluorescence confocal microscopy. Moreover, the number of CYP11B2 immunoreactive DRG neurons co-expressed with aldosterone or MR was significantly increased following painful FCA-induced hind paw inflammation (Mohamed et al., 2020). The results of my work agree with the previous studies by Wang et al.(2016), reporting that the activation of neouronal cells within the hypothalamus by the intra-supraoptic nucleus infusion of angiotensin II upregulates CYP11B2 expression, which leads to an up-regulation of neuronal aldosterone production. Moreover, the aldosterone processing enzyme CYP11B2 mRNA detected in specific neurons in the brain, cortex, cerebellum, brain stem, hippocampus, hypothalamus and amygdala suggests that aldosterone exists and is synthesized within the central nervous system (Davies & Mackenzie, 2003). Since i.t. infusion of the aldosterone synthase inhibitor FAD286 restored the aldosterone concentration in the DRG of inflamed rats compared to that of the controls, the present findings support the local production of aldosterone within sensory DRG neurons under inflammatory conditions (Mohamed et al., 2020). Previous studies, using FAD286, have consistently proved that aldosterone is produced in neurons within the central nervous system (Gomez-Sanchez et al., 2010; Huang et al., 2008). The authors showed that FAD286 significantly

and reversibly lowered enhanced aldosterone content within the brain in the hypertension of Dahl salt-sensitive rats (Gomez-Sanchez et al., 2010; Huang et al., 2008).

In summary, the work in my thesis demonstrates the presence of aldosterone synthase CYP11B2 protein by western blot and mRNA by PCR in DRG neurons. Moreover, the immunohistochemical staining clearly shows that the majority of cells expressing MR with its endogenous ligand aldosterone and the processing enzyme aldosterone synthase in DRG are sensory neurons. Moreover, the protein aldosterone synthase was significantly increased concomitant with the enhanced aldosterone content in MR-ir DRG neurons following local painful inflammation. Importantly, inhibition of the aldosterone synthase in sensory DRG neurons significantly reduced aldosterone content. These findings provide evidence for the local production of aldosterone via aldosterone synthase within peripheral sensory DRG neurons.

6. References

Al-Madol, M. A., Shaqura, M., John, T., Likar, R., Ebied, R. S., Schäfer, M., & Mousa, S. A. (2017). Comparative expression analyses of pro-versus anti-inflammatory mediators within synovium of patients with joint trauma, osteoarthritis, and rheumatoid arthritis. Mediators of Inflammation, 2017. https://doi.org/10.1155/2017/9243736

Barnes, P. J., Adcock, I., Spedding, M., & Vanhoutte, P. M. (1993). Anti-inflammatory actions of steroids: molecular mechanisms. Trends in Pharmacological Sciences, 14(12), 436–441. https://doi.org/10.1016/0165-6147(93)90184-L

Booth, R. E., Johnson, J. P., & Stockand, J. D. (2002). Classical model of aldosterone action. Advances in Physiology Education, 26(1), 8–20.

Capponi, A. M. (2004). The control by angiotensin II of cholesterol supply for aldosterone biosynthesis. Molecular and Cellular Endocrinology, 217(1–2), 113–118. https://doi.org/10.1016/j.mce.2003.10.055

Chalecka-Franaszek, E. H. B. W., & Cote, T. E. (1996). Solubilization of high affinity, guanine nucleotide- sensitive μ-opioid receptors from rat brain membranes. J. Neurochem. 66 (3), 1042e1050, 66(3), 1042–1050.

Chapman, K., Holmes, M., & Seckl, J. (2013). 11B-Hydroxysteroid dehydrogenases intracellular gate-keepers of tissue glucocorticoid action. Physiological Reviews, 93(3), 1139–1206. https://doi.org/10.1152/physrev.00020.2012

Colombo, L., Valle, L. ., Fiore, C., & et al. (2006). Aldosterone and the conquest of land. Endocrinol Invest.

Connell, J. M. C., & Davies, E. (2005). The new biology of aldosterone. Journal of Endocrinology, 186(1), 1–20. https://doi.org/10.1677/joe.1.06017

Davies, E., & Mackenzie, S. M. (2003). Extra-adrenal production of corticosteroids. July 2002, 437–445.

De Kloet, E. R., Van Acker, S. A. B. E., Sibug, R. M., Oitzl, M. S., Meijer, O. C., Rahmouni, K., & De Jong, W. (2000a). Brain mineralocorticoid receptors and centrally regulated functions. Kidney International, 57(4), 1329–1336. https://doi.org/10.1046/j.1523-1755.2000.00971.x

De Kloet, E. R., Van Acker, S. A. B. E., Sibug, R. M., Oitzl, M. S., Meijer, O. C., Rahmouni, K., & De Jong, W. (2000b). Brain mineralocorticoid receptors and centrally regulated functions. Kidney International, 57(4), 1329–1336. https://doi.org/10.1046/j.1523-1755.2000.00971.x

De Oliveira, G. S., Almeida, M. D., Benzon, H. T., & McCarthy, R. J. (2011). Perioperative single dose systemic dexamethasone for postoperative pain: A meta-analysis of randomized controlled trials. Anesthesiology, 115(3), 575–588. https://doi.org/10.1097/ALN.0b013e31822a24c2

Dong, F., & Xie, W. (2012). Reduces Pain Behaviors In Vivo and Decreases Local Inflamed Dorsal Root Ganglia In Vitro. 5, 1102–1112.

Elise Gomez-Sanchez, & Celso E. Gomez-Sanchez. (2014). The multifaceted mineralocorticoid receptor. Compr Physiol, 4(3), 965–994. https://doi.org/10.1016/j.physbeh.2017.03.040

Fleury, A., Mathieu, A. P., Ducharme, L., Hales, D. B., & Lehoux, J. G. (2004). Phosphorylation and function of the hamster adrenal steroidogenic acute regulatory protein (StAR). Journal of Steroid Biochemistry and Molecular Biology, 91(4–5), 259–271. https://doi.org/10.1016/j.jsbmb.2004.04.010

Furukawa, A., Miyatake, A., Ohnishi, T., & Ichikawa, Y. (1998). Steroidogenic acute regulatory protein (StAR) transcripts constitutively expressed in the adult rat central nervous: System: Colocalization of StAR, cytochrome P-450(SCC) (CYP XIA1), and 3β-hydroxysteroid dehydrogenase in the rat brain. Journal of Neurochemistry, 71(6), 2231–2238. https://doi.org/10.1046/j.1471-4159.1998.71062231.x

Gardner, D., & Shoback, D. (2017). (Greenspan's Basic & Clinical Endocrinology) 10th Edition. Greenspan's Basic and Clinical Endocrinology, Tenth Edition, 10th, 944. https://accessmedicine.mhmedical.com/book.aspx?bookID=2178

Garg, N., Perry, L., & Deodhar, A. (2014). Intra-articular and soft tissue injections, a systematic review of relative efficacy of various corticosteroids. Clinical Rheumatology, 33(12), 1695–1706. https://doi.org/10.1007/s10067-014-2572-8

Gomez-Sanchez, E. P., Gomez-Sanchez, C. M., Plonczynski, M., & Gomez-Sanchez, C. E. (2010). Aldosterone synthesis in the brain contributes to Dahl salt-sensitive rat hypertension. Experimental Physiology, 95(1), 120–130. https://doi.org/10.1113/expphysiol.2009.048900

Grafte-Faure, S., Leveque, C., Vasse, M., Soria, C., Norris, V., & Vannier, J. P. (1999). Effects of glucocorticoids and mineralocorticoids on proliferation and maturation of human peripheral blood stem cells. American Journal of Hematology, 62(2), 65–73. https://doi.org/10.1002/(SICI)1096-8652(199910)62:2<65::AID-AJH1>3.0.CO;2-G

Groeneweg, F. L., Karst, H., de Kloet, E. R., & Joëls, M. (2011). Rapid non-genomic effects of corticosteroids and their role in the central stress response. Journal of Endocrinology, 209(2), 153–167. https://doi.org/10.1530/JOE-10-0472

Gu, X. P., Peng, L., Yang, D., Ma, Q., Zheng, Y., Liu, C., Zhu, B., Song, L., Sun, X., & Ma, Z. (2011). The respective and interaction effects of spinal GRs and MRs on radicular pain induced by chronic compression of the dorsal root ganglion in the rat. Brain Research, 1396, 88–95. https://doi.org/10.1016/j.brainres.2011.04.012

Habib, G. S., Saliba, W., & Nashashibi, M. (2010). Local effects of intra-articular corticosteroids. Clinical Rheumatology, 29(4), 347–356. https://doi.org/10.1007/s10067-009-1357-y

Haque, M., Wilson, R., Sharma, K., Mills, N. J., & Teruyama, R. (2015). Localisation of 11β-hydroxysteroid dehydrogenase type 2 in mineralocorticoid receptor expressing magnocellular neurosecretory neurones of the rat supraoptic and paraventricular nuclei. Journal of Neuroendocrinology, 27(11), 835–849. https://doi.org/10.1111/jne.12325

Herrada, A. A., Campino, C., Amador, C. A., Michea, L. F., Fardella, C. E., & Kalergis, A. M. (2011). Aldosterone as a modulator of immunity: Implications in the organ damage. Journal of Hypertension, 29(9), 1684–1692. https://doi.org/10.1097/HJH.0b013e32834a4c75

Huang, B. S., White, R. A., Ahmad, M., Jeng, A. Y., & Leenen, F. H. H. (2008). Central infusion of aldosterone synthase inhibitor prevents sympathetic hyperactivity and hypertension by central Na+ in Wistar rats. American Journal of Physiology - Regulatory Integrative and Comparative Physiology, 295(1), 166–172. https://doi.org/10.1152/ajpregu.90352.2008

Konosu-Fukaya, S., Nakamura, Y., Satoh, F., Felizola, S. J. A., Maekawa, T., Ono, Y., Morimoto, R., Ise, K., Takeda, K. ichiro, Katsu, K., Fujishima, F., Kasajima, A., Watanabe, M., Arai, Y., Gomez-Sanchez, E. P., Gomez-Sanchez, C. E., Doi, M., Okamura, H., & Sasano, H. (2015). 3B-hydroxysteroid dehydrogenase isoforms in human aldosterone-producing adenoma. Molecular and Cellular Endocrinology, 408, 205–212.

https://doi.org/10.1016/j.mce.2014.10.008

Li, X., Shaqura, M., Ph, D., Mohamed, D., Beyer, A., Yamada, S., Ph, D., Mousa, S. A., Ph, D., Schäfer, M., & Ph, D. (2018). Pro-versus antinociceptive nongenomic effects of neuronal mineralocorticoid versus glucocorticoid receptors during rat hind paw inflammation. Anesthesiology, 128(4). https://doi.org/10.1097/ALN.0000000000002087.

Lockett, B. Y. M. F., & Retallack, R. W. (1970). The influence of heart rate on the i8-monoacetate of d-aldosterone by the hearts of cats under chloralose anaesthesia. From the Department of Pharmacology , The University of of only 22-5 + 1-76 beats / min doubled the concentration of HS when the. 21–32.

Lombès, M., Alfaidy, N., Eugene, E., Lessana, A., Farman, N., & Bonvalet, J.-P. (1995). Prerequisite for cardiac aldosterone action. Circulation, 92(2), 175–182. https://doi.org/10.1161/01.cir.92.2.175

MacKenzie, S. M., Connell, J. M. C., & Davies, E. (2012). Non-adrenal synthesis of aldosterone: A reality check. Molecular and Cellular Endocrinology, 350(2), 163–167. https://doi.org/10.1016/j.mce.2011.06.026

Mahmood, T., & Yang, P. C. (2012). Western blot: Technique, theory, and trouble shooting. North American Journal of Medical Sciences, 4(9), 429–434. https://doi.org/10.4103/1947-2714.100998

Manders, E. M. M., VERBEEK, F. J., & ATEN, J. A. (1993). Measurement of co-localization of objects in dual-colour confocal images. Journal of Microscopy, 169(3), 375–382. https://doi.org/10.1111/j.1365-2818.1993.tb03313.x

Mizuno, Y., Yoshimura, M., Yasue, H., Sakamoto, T., Ogawa, H., Kugiyama, K., Harada, E., Nakayama, M., Nakamura, S., Ito, T., Shimasaki, Y., Saito, Y., & Nakao, K. (2001). Aldosterone production is activated in failing ventricle in humans. Circulation, 103(1), 72–77. https://doi.org/10.1161/01.CIR.103.1.72

Mohamed, D. M., Shaqura, M., Li, X., Shakibaei, M., Beyer, A., Treskatsch, S., Schäfer, M., & Mousa, S. A. (2020). Aldosterone synthase in peripheral sensory neurons

contributes to mechanical hypersensitivity during local inflammation in rats. Anesthesiology, Xxx, 867–880. https://doi.org/10.1097/ALN.0000000000003127

Monticone, S., Rainey, W. E., Bollag, W. B., & Isales, C. M. (2018). Regulation of aldosterone production. Textbook of Nephro-Endocrinology, 429–449. https://doi.org/10.1016/b978-0-12-803247-3.00025-8

Mousa, S. A., Shaqura, M., Winkler, J., Khalefa, B. I., Al-Madol, M. A., Shakibaei, M., Schulz, S., & Schäfer, M. (2016). Protein kinase C-mediated mu-opioid receptor phosphorylation and desensitization in rats, and its prevention during early diabetes. Pain, 157(4), 910–921. https://doi.org/10.1097/j.pain.0000000000000459

Mousa, S. A., Straub, R. H., Schäfer, M., & Stein, C. (2007). β-Endorphin, Met-enkephalin and corresponding opioid receptors within synovium of patients with joint trauma, osteoarthritis and rheumatoid arthritis. Annals of the Rheumatic Diseases, 66(7), 871–879. https://doi.org/10.1136/ard.2006.067066

Muñoz-Durango, N., Vecchiola, A., Gonzalez-Gomez, L. M., Simon, F., Riedel, C. A., Fardella, C. E., & Kalergis, A. M. (2015). Modulation of immunity and inflammation by the Mineralocorticoid receptor and Aldosterone. BioMed Research International, 2015. https://doi.org/10.1155/2015/652738

Rittner, H. L., Brack, A., Machelska, H., Mousa, S. A., Bauer, M., Schäfer, M., & Stein, C. (2001). Opioid Peptide – expressing Leukocytes. Anesthesiology 2001, 95:500–508.

Rossignol, P., Ménard, J., Fay, R., Gustafsson, F., Pitt, B., & Zannad, F. (2011). Eplerenone survival benefits in heart failure patients post-myocardial infarction are independent from its diuretic and potassium-sparing effects: Insights from an EPHESUS (Eplerenone Post-Acute Myocardial Infarction Heart Failure Efficacy and Survival St. Journal of the American College of Cardiology, 58(19), 1958–1966. https://doi.org/10.1016/j.jacc.2011.04.049

Shaqura, M., Khalefa, B. I., Shakibaei, M., Winkler, J., Al-Khrasani, M., Fürst, S., Mousa, S. A., & Schäfer, M. (2013). Reduced number, G protein coupling, and antinociceptive efficacy of spinal mu-opioid receptors in diabetic rats are reversed by nerve growth

factor. Journal of Pain, 14(7), 720–730. https://doi.org/10.1016/j.jpain.2013.01.776

Shaqura, M., Li, X., Al-Khrasani, M., Shakibaei, M., Tafelski, S., Fürst, S., Beyer, A., Kawata, M., Schäfer, M., & Mousa, S. A. (2016). Membrane-bound glucocorticoid receptors on distinct nociceptive neurons as potential targets for pain control through rapid non-genomic effects. Neuropharmacology, 111, 1–13. https://doi.org/10.1016/j.neuropharm.2016.08.019

Shaqura, M., Li, X., Al-Madol, M. A., Tafelski, S., Beyer-Koczorek, A., Mousa, S. A., & Schäfer, M. (2016). Acute mechanical sensitization of peripheral nociceptors by aldosterone through non-genomic activation of membrane bound mineralocorticoid receptors in naive rats. Neuropharmacology, 107, 251–261. https://doi.org/10.1016/j.neuropharm.2016.03.032

Slight, S. H., Ganjam, V. K., Gómez-Sánchez, C. E., Zhou, M. Y., & Weber, K. T. (1996). High affinity NAD+-dependent 11 β-hydroxysteroid dehydrogenase in the human heart. Journal of Molecular and Cellular Cardiology, 28(4), 781–787. https://doi.org/10.1006/jmcc.1996.0072

Sun, Y. e., Peng, L., Sun, X., Bo, J., Yang, D., Zheng, Y., Liu, C., Zhu, B., Ma, Z., & Gu, X. (2012). Intrathecal injection of spironolactone attenuates radicular pain by inhibition of spinal microglia activation in a rat model. PLoS ONE, 7(6), 1–10. https://doi.org/10.1371/journal.pone.0039897

Testas, I. J., Hu, Z. Y., Baulieu, E. E., & Robel, A. P. (1989). Neurosteroids: Biosynthesis of pregnenolone and progesterone in primary cultures of rat glial cells. Endocrinology, 125(4), 2083–2091. https://doi.org/10.1210/endo-125-4-2083

van Steensel, B., van Binnendijk, E. P., Hornsby, C. D., van der Voort, H. T. M., Krozowski, Z. S., de Kloet, E. R., & van Driel, R. (1996). Discrete Compartments in Nuclei of Rat Hippocampus Neurons. Journal of Cell Science, 109, 787–792.

Wang, H. W., Huang, B. S., White, R. A., Chen, A., Ahmad, M., & Leenen, F. H. H. (2016). Mineralocorticoid and angiotensin II type 1 receptors in the subfornical organ mediate angiotensin II - induced hypothalamic reactive oxygen species and

hypertension. Neuroscience, 329, 112–121. https://doi.org/10.1016/j.neuroscience.2016.04.050

Ye, L., Xie, W., Strong, J. A., & Zhang, J. M. (2014). Blocking the mineralocorticoid receptor improves effectiveness of steroid treatment for low back pain in rats. Anesthesiology, 121(3), 632–643. https://doi.org/10.1097/ALN.0000000000000277

Yoshimura, M., Nakamura, S., Ito, T., Nakayama, M., Harada, E., Mizuno, Y., Sakamoto, T., Yamamuro, M., Saito, Y., Nakao, K., Yasue, H., & Ogawa, H. (2002). Expression of aldosterone synthase gene in failing human heart: Quantitative analysis using modified real-time polymerase chain reaction. Journal of Clinical Endocrinology and Metabolism, 87(8), 3936–3940. https://doi.org/10.1210/jcem.87.8.8731

Zhang, Z. H., Kang, Y. M., Yu, Y., Wei, S. G., Schmidt, T. J., Johnson, A. K., & Felder, R. B. (2006). 11B-Hydroxysteroid Dehydrogenase Type 2 Activity in Hypothalamic Paraventricular Nucleus Modulates Sympathetic Excitation. Hypertension, 48(1), 127–133. https://doi.org/10.1161/01.HYP.0000224296.96235.dd

7. Statutory Declaration

"I, Doaa M. Mohamed, by personally signing this document in lieu of an oath, hereby affirm that I prepared the submitted dissertation on the topic [The role of neuronal steroid receptors and endogenous ligands in pain modulation], independently and without the support of third parties, and that I used no other sources and aids than those stated.

All parts, which are based on the publications or presentations of other authors, either in letter or in spirit, are specified as such in accordance with the citing guidelines. The sections on methodology (in particular regarding practical work, laboratory regulations, statistical processing) and results (in particular regarding figures, charts and tables) are exclusively my responsibility.

Furthermore, I declare that I have correctly marked all of the data, the analyses, and the conclusions generated from data obtained in collaboration with other persons, and that I have correctly marked my own contribution and the contributions of other persons (cf. declaration of contribution). I have correctly marked all texts or parts of texts that were generated in collaboration with other persons.

My contributions to any publications to this dissertation correspond to those stated in the below joint declaration made together with the supervisor. All publications created within the scope of the dissertation comply with the guidelines of the ICMJE (International Committee of Medical Journal Editors; www.icmje.org) on authorship. In addition, I declare that I shall comply with the regulations of Charité – Universitätsmedizin Berlin on ensuring good scientific practice.

I declare that I have not yet submitted this dissertation in identical or similar form to another Faculty.

The significance of this statutory declaration and the consequences of a false statutory declaration under criminal law (Sections 156, 161 of the German Criminal Code) are known to me."

Date: ---------- ----------

Doaa Mohamed

8. Declaration of my own contribution to the top-journal publication for a PhD degree

Doaa Mohamed contributed the following to the below listed publication:

Doaa Mohamed, Mohammed Shaqura, Xiongjuan Li, Mehdi Shakibaei, Antje Beyer, Sascha Treskatsch, Michael Schäfer, Shaaban A. Mousa; **Aldosterone Synthase in Peripheral Sensory Neurons Contributes to Mechanical Hypersensitivity during Local Inflammation in Rats**. **Anesthesiology** 2020; 132(4): 867- 88

I, Doaa Mohamed, by personally signing this document, hereby affirm that I contributed to all immunohistochemical and western blot experiments. I collected the tissue, prepared the tissue sections for the experiments, administered all required antibodies and performed all quantifications. In addition, I participated in sacrificing the animals to obtain tissue of the dorsal root ganglia. I analysed the respective data obtained from my experiments, performed the statistical tests, and wrote part of the methods and results section. The Fig. 2C, D and Fig. 2E-M, Fig. 3A-E, Fig. 4E-F, Fig. 5 and Fig. 7A-E were created by me and were based on my statistical evaluations. Finally, I contributed to the introduction and discussion of the manuscript, revised the final draft and approved the final version of the manuscript.

Unterschrift, Datum und Stempel des betreuenden Hochschullehrers

---

Prof. Dr. med. Michael Schäfer

Unterschrift des Doktoranden

Doaa Mohamed

9. Journal Data Filtered By: **Selected JCR Year: 2017** Selected Editions: SCIE,SSCI Selected Categories: **"ANESTHESIOLOGY"** Selected Category Scheme: WoS

Gesamtanzahl: 31 Journale

Rank	Full Journal Title	Total Cites	Journal Impact Factor	Eigenfactor Score
1	ANESTHESIOLOGY	28,896	6.523	0.029600
2	BRITISH JOURNAL OF ANAESTHESIA	20,435	6.499	0.026390
3	PAIN	36,132	5.559	0.038000
4	ANAESTHESIA	10,098	5.431	0.009760
5	REGIONAL ANESTHESIA AND PAIN MEDICINE	4,732	4.382	0.005510
6	EUROPEAN JOURNAL OF ANAESTHESIOLOGY	4,097	3.958	0.005110
7	ANESTHESIA AND ANALGESIA	26,298	3.463	0.021980
8	INTERNATIONAL JOURNAL OF OBSTETRIC ANESTHESIA	1,681	3.404	0.002050
9	Canadian Journal of Anesthesia-Journal canadien d anesthesie	5,595	3.377	0.005660
10	JOURNAL OF NEUROSURGICAL ANESTHESIOLOGY	1,607	3.238	0.002370
11	CLINICAL JOURNAL OF PAIN	6,585	3.209	0.010350
12	EUROPEAN JOURNAL OF PAIN	6,537	2.991	0.010320
13	PAIN MEDICINE	6,123	2.782	0.012240
14	Minerva Anestesiologica	2,589	2.693	0.004190
15	Current Opinion in Anesthesiology	2,722	2.581	0.004030
16	Pain Physician	3,848	2.556	0.007290
17	JOURNAL OF CLINICAL MONITORING AND COMPUTING	1,605	2.450	0.002970
18	PEDIATRIC ANESTHESIA	4,953	2.389	0.006170
19	ACTA ANAESTHESIOLOGICA SCANDINAVICA	7,065	2.270	0.007340
20	Anaesthesia Critical Care & Pain Medicine	245	2.200	0.000640
21	Pain Practice	2,046	2.187	0.004420
22	JOURNAL OF CLINICAL ANESTHESIA	3,442	1.818	0.003790
23	BMC Anesthesiology	1,238	1.788	0.003720
24	ANAESTHESIA AND INTENSIVE CARE	2,730	1.702	0.003080

Rank	Full Journal Title	Total Cites	Journal Impact Factor	Eigenfactor Score
25	JOURNAL OF CARDIOTHORACIC AND VASCULAR ANESTHESIA	4,179	1.574	0.006660
26	Journal of Anesthesia	2,111	1.454	0.003500
27	SCHMERZ	816	1.215	0.000850
28	ANAESTHESIST	1,359	0.995	0.001100
29	ANASTHESIOLOGIE & INTENSIVMEDIZIN	341	0.880	0.000240
30	Revista Brasileira de Anestesiologia	836	0.850	0.001180
31	ANASTHESIOLOGIE INTENSIVMEDIZIN NOTFALLMEDIZIN SCHMERZTHERAPIE	374	0.262	0.000230

ANESTHESIOLOGY

Aldosterone Synthase in Peripheral Sensory Neurons Contributes to Mechanical Hypersensitivity during Local Inflammation in Rats

Doaa M. Mohamed, M.Sc., Mohammed Shaqura, Ph.D., Xiongjuan Li, M.D., Mehdi Shakibaei, Ph.D., Antje Beyer, M.D., Sascha Treskatsch, M.D., Michael Schäfer, M.D., Ph.D., Shaaban A. Mousa, Ph.D.

ANESTHESIOLOGY 2020; XXX:00–00

EDITOR'S PERSPECTIVE

What We Already Know about This Topic

- Aldosterone is believed to be synthesized exclusively in the adrenal gland through the processing enzyme aldosterone synthase
- Mineralocorticoid receptors are predominantly expressed in peripheral nociceptive neurons whose activation leads to increased neuronal excitability and mechanical sensitivity

What This Article Tells Us That Is New

- Extra-adrenal production of aldosterone by aldosterone synthase within peripheral sensory neurons contributes to ongoing mechanical hypersensitivity *via* intrinsic activation of neuronal mineralocorticoid receptors
- Intrathecally-applied aldosterone synthase inhibitor reduced aldosterone content in peripheral sensory neurons and subsequently attenuated enhanced mechanical hypersensitivity resulting from local inflammation

ABSTRACT

Background: Recent emerging evidence suggests that extra-adrenal synthesis of aldosterone occurs (*e.g.*, within the failing heart and in certain brain areas). In this study, the authors investigated evidence for a local endogenous aldosterone production through its key processing enzyme aldosterone synthase within peripheral nociceptive neurons.

Methods: In male Wistar rats (n = 5 to 8 per group) with Freund's complete adjuvant hind paw inflammation, the authors examined aldosterone, aldosterone synthase, and mineralocorticoid receptor expression in peripheral sensory neurons using quantitative reverse transcriptase–polymerase chain reaction, Western blot, immunohistochemistry, and immunoprecipitation. Moreover, the authors explored the nociceptive behavioral changes after selective mineralocorticoid receptor antagonist, canrenoate-K, or specific aldosterone synthase inhibitor application.

Results: In rats with Freund's complete adjuvant–induced hind paw inflammation subcutaneous and intrathecal application of mineralocorticoid receptor antagonist, canrenoate-K, rapidly and dose-dependently attenuated nociceptive behavior (94 and 48% reduction in mean paw pressure thresholds, respectively), suggesting a tonic activation of neuronal mineralocorticoid receptors by an endogenous ligand. Indeed, aldosterone immunoreactivity was abundant in peptidergic nociceptive neurons of dorsal root ganglia and colocalized predominantly with its processing enzyme aldosterone synthase and mineralocorticoid receptors. Moreover, aldosterone and its synthesizing enzyme were significantly upregulated in peripheral sensory neurons under inflammatory conditions. The membrane mineralocorticoid receptor consistently coimmunoprecipitated with endogenous aldosterone, confirming a functional link between mineralocorticoid receptors and its endogenous ligand. Importantly, inhibition of endogenous aldosterone production in peripheral sensory neurons by a specific aldosterone synthase inhibitor attenuated nociceptive behavior after hind paw inflammation (a 32% reduction in paw pressure thresholds; inflammation, 47 ± 2 [mean ± SD] *vs.* inflammation + aldosterone synthase inhibitor, 62 ± 2).

Conclusions: Local production of aldosterone by its processing enzyme aldosterone synthase within peripheral sensory neurons contributes to ongoing mechanical hypersensitivity during local inflammation *via* intrinsic activation of neuronal mineralocorticoid receptors.

(ANESTHESIOLOGY 2020; XXX:00–00)

Aldosterone is known to regulate the body's water and electrolyte balance through activation of corresponding mineralocorticoid receptors on epithelial cells of the renal cortical collecting ducts leading to sodium and water retention in exchange for excreted potassium.[1,2] Aldosterone is generated and secreted in the zona glomerulosa of the adrenal gland through local aldosterone synthase (CYP11B2).[1] Aldosterone circulates in the blood unbound (30 to 50% of total aldosterone) or bound to albumin- or corticosteroid-binding globulin (50 to 70% of total aldosterone). It is rapidly inactivated in the liver with a plasma half-life of 15 to 20 min.[3] While initial reports of aldosterone production outside the adrenal glands were challenged,[4] Takeda and others identified

D.M.M. and M. Shaqura contributed equally to this article.

Submitted for publication April 5, 2019. Accepted for publication December 10, 2019. From the Department of Anaesthesiology and Intensive Care Medicine, Charite Campus Benjamin Franklin, Charité – Universitätsmedizin Berlin, Berlin, Germany (D.M.M., M. Shaqura, X.L., S.T., M. Schäfer, S.A.M.); Department of Zoology, Faculty of Science, Aswan University, Aswan, Egypt (D.M.M.); and the Departments of Anatomy (M. Shakibaei) and Anaesthesiology (A.B.), Ludwig Maximilian University of Munich, Munich, Germany.

 Anesthesiology 2020; XXX:00–00. DOI: 10.1097/ALN.0000000000003127

aldosterone synthase (CYP11B2) mRNA expression and aldosterone synthesis in rodent cardiovascular tissue.[5,6] This was later confirmed for the failing human heart, as well.[7,8] More recently, further evidence for extra-adrenal aldosterone synthesis has been demonstrated for specific neurons within the brain (*e.g.,* the hypothalamus and rostral ventral medulla) at which aldosterone appears to contribute to the depolarization of neurons.[9–12] Recent functional evidence implies aldosterone may also play a role in the peripheral nervous system. In an animal model of chronic lumbar dorsal root ganglia compression intrathecal aldosterone antagonism *via* delivery of spironolactone-reversed mechanical allodynia 2 days postsurgery.[13] In the same animal model, the antiallodynic effect of intrathecal spironolactone 4 and 7 days postsurgery paralleled the attenuation of spinal microglia activation and cytokine production.[14] In the rat model of zymosan-induced L5 dorsal root ganglion inflammation 500 μg of the mineralocorticoid receptor antagonist eplerenone given to the site of dorsal root ganglia inflammation reversed mechanical allodynia 1 to 13 days after intervention.[2,15] These effects occurred within days and were considered to be genomic, either through a reversal of nuclear mineralocorticoid receptor translocation or through attenuation of satellite cell activation.[2,15] More recently, we identified mineralocorticoid receptors predominantly on the subpopulation of peptidergic unmyelinated nociceptive C-fibers, strongly indicating a role for the modulation of nociception.[16] Indeed, local application of the mineralocorticoid receptor agonist aldosterone at the peripheral and central nerve terminals of nociceptive neurons elicited a rapid increased mechanical sensitivity.[16] Consistent with this pronociceptive effect, previous studies have shown that aldosterone increased the number of action potentials that were evoked in acutely dissociated dorsal root ganglion neurons.[2,15,17] These effects occurred rapidly, were most likely due to nongenomic mechanisms, and were mediated by membrane-bound mineralocorticoid receptors which were identified by membrane saturation binding.[16]

Using the animal model of unilateral Freund's complete adjuvant hind paw inflammation, this study investigated whether: (1) the antagonism of mineralocorticoid receptors on peripheral sensory neurons will result in the attenuation of mechanical hyperalgesia, suggesting an intrinsic tone of endogenous aldosterone; (2) peripheral sensory neurons are a potential source for local aldosterone production; (3) aldosterone is coexpressed with its processing enzyme aldosterone synthase and if their expression is upregulated during inflammatory conditions; (4) there is a functional link between endogenous aldosterone and sensory neuron mineralocorticoid receptors; and (5) the inhibition of aldosterone's production in peripheral sensory neurons by local administration of a specific aldosterone synthase inhibitor will result in the attenuation of mechanical hypersensitivity. The overall hypothesis, therefore, is that antagonism of sensory neuron mineralocorticoid receptors attenuates inflammation-induced mechanical hyperalgesia most likely due to the inhibition of an endogenous tonic activation through aldosterone derived from peripheral sensory neurons. This would have implications for similar human conditions (*e.g.,* arthritis, vertebral disc herniation) that an ongoing endogenous activation of mineralocorticoid receptors might contribute to enhanced mechanical sensitivity.

Materials and Methods

Drugs

Freund's complete adjuvant, a water-in-oil emulsion with killed mycobacteria (Calbiochem, USA); canrenoate-K, and aldosterone synthase inhibitor (FAD286; Sigma-Aldrich, USA) were dissolved in 0.9% NaCl as described previously.[18,19] Drugs were administered subcutaneously in a volume of 1 ml/kg body weight or intrathecally in a volume of 20 μl. Subcutaneous injections were given under the loose skin of the back, just behind and between the shoulder blades.

Animals

Experiments were conducted in male Wistar rats (180 to 250 g; breeding facility: Charité-Universitätsmedizin, Germany) after approval by the local animal care committee and according to the European Directive for animal welfare and care guidelines (2010/63/EU). Wistar rats were anesthetized by brief isoflurane anesthesia and followed by an intraplantar injection of 0.15 ml Freund's complete adjuvant (Calbiochem) into the right hind paw. This treatment consistently produces a local inflammation of the inoculated paw characterized by an increase in paw volume and temperature, mechanical hypersensitivity, and infiltration of various types of immune cells.[20] All experiments were performed between 10:00 AM and 2:00 PM on the fourth day of Freund's complete adjuvant hind paw inflammation.

For continuous intrathecal delivery of drugs, animals were implanted with chronic intrathecal catheters, as described previously by Shaqura *et al.*[21] Briefly, animals were anesthetized with isoflurane in oxygen *via* nose cone. A longitudinal skin incision was made in the lumbar region directly above the spinous processes of the L4–L6 vertebrae. The needle through which the catheter (PE 10 tubing attached to PE 60 tubing for attachment to an osmotic pump; Portex Ltd, United Kingdom) was set up, was inserted at a 30° angle between the L5 and L6 vertebra. Then, the catheter was carefully advanced upward 1 cm into the intrathecal space while rotating it between the thumb and forefinger. The sign of dura penetration was observed by involuntary movements of the tail or hind limb. Finally, the correct location of the catheter was verified by 10 μl lidocaine 2%, which caused reversible bilateral hind limb paresis for 10 to 15 min.

Experimental Protocols

The first set of experiments examined the influence of 4 days of Freund's complete adjuvant hind paw inflammation on changes in the neuronal aldosterone, aldosterone synthase, 11β-hydroxysteroid-dehydrogenase 2, and mineralocorticoid receptor expression in the innervating dorsal root ganglia. Subsequent experiments assessed the impact of systemic (5 to 20 mg/kg) or intrathecal (10 to 100 μg in 20 μl) injections of increasing doses of mineralocorticoid receptor antagonist, canrenoate-K, on mechanical paw pressure thresholds. The doses chosen for canrenoate-K were based on our previous studies.[19,22] A final set of experiments investigated at 4 days of Freund's complete adjuvant hind paw inflammation the effects of the intrathecal delivery of the aldosterone synthase inhibitor, FAD286, on both aldosterone content and on mechanical paw pressure thresholds. Rats received the following intrathecal treatments for more than 5 days, beginning 1 day before Freund's complete adjuvant–induced inflammation. For intrathecal FAD286 delivery, Alzet osmotic minipumps (2 ml; rate, 5.0 μl/h; Alzet Corporation, USA) were filled with 0.9% NaCl with or without FAD286 (100 $\mu g \cdot kg^{-1} \cdot day^{-1}$) and connected to the intrathecal catheter to administer FAD286 or the vehicle continuously at 5.0 μl/h.[23] All tests were performed on day 5 after pump implantation.

Mechanical Hyperalgesia Testing

The mechanical hyperalgesia following Freund's complete adjuvant–induced hind paw inflammation was assessed by a pressure apparatus (Ugo-Basile SRL, Italy) with increasing force (measured in grams) applied to the plantar hind paw until a withdrawal reflex was precipitated as described previously.[19] A 250-g cut-off value was assigned in the absence of a response. Mechanical paw pressure tests were performed on the fourth day of Freund's complete adjuvant–induced hind paw inflammation before (baseline) and after drug application. Subsequently, mechanical paw pressure thresholds were reassessed at different time points (0 to 120 min) after drug administrations to determine drug-related behavior. Each measurement was performed three times consecutively with a time interval of at least 15 s before the next stimulus was applied. In all behavioral experiments, drugs were prepared by a different person (M. Shakibaei), and the examiner (X.L.) was unaware (*i.e.*, blinded) of the treatment that each animal had received. Animals were incidentally allocated to treatments; however, no specific randomization method was used to assign animals to condition.

11β-Hydroxysteroid-Dehydrogenase and Aldosterone Synthase mRNA Detection by TaqMan Quantitative Polymerase Chain Reaction

Total RNA extracted from L3–L5 dorsal root ganglia of Wistar rats using RNeasy Kit (Qiagen, Germany), as previously described,[19,24] was subjected to the TaqMan quantitative polymerase chain reaction using an SYBR Green kit following the manufacturer's instructions (Thermo Fisher Scientific, Germany). The products were amplified using aldosterone synthase CYP11B2 specific primers: forward primer, 5'-TGGCAGCACTAATAACTCAGGG-3'; reverse primer, 5'-ATTGCTGTCGTGTCAACGCT-3' (Ensemble, Accession No: NM_012538.2); for 11β-hydroxysteroid-dehydrogenase: forward primer, 5'-CGCCGC TTCCTACAGAACTT-3'; reverse primer, 5'-TCCTGGGTTGTGTCATGAACA-3' (Ensemble Accession No: NM_017081.2). Amplification was performed with 40 cycles, each consisting of 15 s at 95°C. The gene-specific fluorescent amplified products were detected just below the determined melting temperature for each product (aldosterone synthase CYP11B2: melting temperature, 83°C; 11β-hydroxysteroid-dehydrogenase: melting temperature, 76°C; 18S: melting temperature, 83°C). Aldosterone synthase and 11β-hydroxysteroid-dehydrogenase mRNA products were quantified in replicates of three samples using the delta-delta Ct method.[19] In addition, the housekeeping gene 18s (Accession No. NR_046237) as the internal reference was quantified using TaqMan quantitative polymerase chain reaction with the following primers: forward primer, CGGCTACCACATCCAAGGAA; reverse primer, GCTGGAATTACCGCGGCT.

Aldosterone Quantification in Plasma and Dorsal Root Ganglia

Blood samples were collected by intracardiac aspiration directly into rapid serum tubes (BD Vacutainer; Becton Dickinson, Germany) from the isoflurane anesthesia sacrificed rats (n = 15, 17). The samples were centrifuged at 1,000 relative centrifugal force and snap frozen at −80°C. These were subsequently subjected to chemiluminescence immunoassay by an external commercial laboratory (SynLab Vet, Germany) to measure the aldosterone plasma concentrations. In parallel, dorsal root ganglia were prepared as previously described,[25,26] in Dulbecco's Modified Eagle Medium (Thermo Fisher Scientific). Briefly, thoracic and lumbar dorsal root ganglia of male Wistar rats (n = 5) were removed and placed in sterile Dulbecco's Modified Eagle's Medium at 4°C. Dorsal root ganglia were digested with collagenase type 2 in Minimum Essential Medium (Biochrom AG, Germany) at 37°C for 50 min, and with 0.025% trypsin for 10 min at 37°C. After digestion, dorsal root ganglia were carefully dissociated by mechanical agitation, and centrifuged at 500 g for 5 min and then at 300 g for 5 min. The cells were maintained overnight in Minimum Essential Medium growth media supplemented with 10% horse serum and 50 μg/ml penicillin and streptomycin, and plated in 24-well microplates (1.9 cm^2) at 37°C in an atmosphere of 5% CO_2. Then, the aldosterone content in dorsal root ganglia was determined by a commercial enzyme-linked immunosorbent

assay (ELISA) kit (cat. no. KGE016; R&D Systems, USA), according to the manufacturer's specifications and our previous study.[19] Measurements were performed independently in five to six rats and in triplicate using the same sample. The optical density for each well was determined using a microplate reader (LS45; Perkin Elmer, USA) set to 450 nm. The mean of triplicate readings for each standard, control, and sample subtracted by the average nonspecific binding optical density were measured. A standard curve was created by generating a four-parameter logistic curve-fit using the computer software (LS45; Perkin Elmer).

Western Blot

Dorsal root ganglia and spinal cords from adult rats were solubilized and extracted for immunoblotting investigations as previously described.[16,24] After blotting, membranes were blocked in 3% bovine serum albumin for 2 h and incubated with mouse anti-aldosterone synthase (1:1,000 in 3% BSA; anti-CYP11B2; Merck Millipore, Germany) or rabbit anti–11β-hydroxysteroid-dehydrogenase 2 (1:500 in 3% BSA; St. John's Laboratory Ltd., United Kingdom) or sheep anti–11β-hydroxysteroid-dehydrogenase 2 (1:200 in 3% BSA; private gift from Dr. Elise Gomez-Sanchez, Department of Pharmacology and Toxicology, University of Mississippi Medical Center, Jackson, Mississippi). After incubation with the secondary antibody (peroxidase-conjugated goat anti-rabbit, 1:40,000; Jackson ImmunoResearch, USA) for 2 h at ambient temperature, reactive protein bands were digitally visualized using enhanced chemiluminescence solutions (SuperSignal West Pico; Thermo Fisher Scientific) in ChemiDoc MP Imager. Finally, the blots were reprobed with monoclonal mouse anti-beta actin antibody (1:20,000; Sigma-Aldrich) as an internal standard. Experiments were performed in groups of four to five animals.

The Western blot bands specific for aldosterone synthase (CYP11B2, 57 kDa) or 11β-hydroxysteroid-dehydrogenase (11β-HSD2, 70 kDa) were quantified by Java Image processing and analysis software (ImageJ, open-source image software downloaded from the web; http://rsb.info.nih.gov/ij/, accessed March 9, 2018).[16,22] The area and density of pixels within the threshold values representing immunoreactivity were measured, and the integrated density (the product of the area and mean of grey values) was calculated. Integrated immunodensities of controls and treated groups were compared and statistically analyzed.[21]

Immunohistochemistry

After transcardial perfusion of rats (4 days after Freund's complete adjuvant inoculation) dorsal root ganglia were removed and processed as described previously.[19,22] Tissue sections were then incubated overnight with the following primary antibodies: polyclonal rabbit anti-aldosterone (1:500; Novus Biologicals, LLC, USA), in combination with a polyclonal guinea pig anti–calcitonin gene-related peptide, monoclonal mouse anti–mineralocorticoid receptor (private gift from Dr. Elise Gomez-Sanchez) or aldosterone synthase (CYP11B2); in addition, polyclonal sheep antibody against 11β-hydroxysteroid-dehydrogenase was examined in combination with the monoclonal mouse anti–mineralocorticoid receptor (private gift from Dr. Elise Gomez-Sanchez). The species, sources, dilutions, and immunogens of the primary antibodies used in this study are summarized in Supplemental Digital Content, table S1 (http://links.lww.com/ALN/C235). Finally, the tissues were washed in phosphate-buffered saline, mounted in Vectashield (Vector Laboratories, USA) and examined by confocal laser scanning microscope (LSM 510, Carl Zeiss, Germany) as described previously.[19] To demonstrate specificity of staining, the following controls were included as previously reported by our group[19,22,24]: omission of either the primary antisera or the secondary antibodies.

The quantification of dorsal root ganglia staining has been described previously.[19,22,24,27] For counting of the total number of neurons, only those immunostained neurons containing a distinct nucleus were counted. In a similar way, the number of aldosterone immunoreactive cells divided by the total number of dorsaal root ganglion cells, the number of mineralocorticoid receptor immunoreactive cells divided by the total number of dorsal root ganglion cells, the number of 11β-hydroxysteroid-dehydrogenase immunoreactive cells divided by the total number of total dorsal root ganglion cells, the number of aldosterone synthase (CYP11B2) immunoreactive cells divided by the total number of total dorsal root ganglion cells, the number of aldosterone plus mineralocorticoid receptor immunoreactive cells divided by the total number of total dorsal root ganglion cells, the number of calcitonin gene–related peptide plus aldosterone immunoreactive cells divided by the total number of total dorsal root ganglion cells, the number of calcitonin gene–related peptide plus aldosterone synthase (CYP11B2) immunoreactive cells divided by the total number of total dorsal root ganglion cells, the number of calcitonin gene–related peptide plus 11β-hydroxysteroid-dehydrogenase immunoreactive cells divided by the total number of total dorsal root ganglion cells, the number of total dorsal root ganglia divided by aldosterone plus aldosterone synthase (CYP11B2) immunoreactive cells divided by the total number of total dorsal root ganglion cells were counted in each dorsal root ganglion section and represented as percentages. Data were obtained from two to three sections per rat and four to five rats per group using 40× objective lens.

Coimmunoprecipitation Assay

L4–L5 dorsal root ganglia samples were solubilized according to Shaqura *et al.*,[28] to obtain whole cell lysate. For quantifying membrane-bound *versus* cytosolic mineralocorticoid receptor, subcellular fractionation was performed as previously described.[23] To examine whether endogenous aldosterone and membranous mineralocorticoid receptor or transmembrane molecule integrin-ß1 integrin as a membrane marker interact with each other, we performed coimmunoprecipitation assays as reported earlier.[29]

Briefly, precleared membrane fraction protein extracts were immunoprecipitated with rabbit polyclonal primary antibody against aldosterone (Novus Biologicals, LLC). Then, immune complexes were subjected to Western blot analysis using mouse monoclonal anti–mineralocorticoid receptor (private gift from Dr. Elise Gomez-Sanchez) or anti–transmembrane ß1-integrin (Merck Millipore).

Statistical Analysis

All tests were performed using Sigma Plot 13.0 software (SPSS Inc., Germany). TaqMan quantitative polymerase chain reaction (unit: fold change in delta-delta CT over control), Western blot (unit: fold change in integrated optical density over control) as well as immunofluorescence data (unit: number of immunoreactive cells) were analyzed as two group comparisons (Freund's complete adjuvant–treated rats *vs.* controls) by the two-tailed independent Student *t* test in case of normally distributed data. Paw pressure thresholds were determined before and after drug injections, expressed as mean ± SD, and statistically analyzed by an independent paired *t* test to examine for differences between baseline values and values obtained 4 days after Freund's complete adjuvant injection or to examine for alterations between different drug doses (between factor analysis) and different time intervals (within factor analysis) by two-way repeated measures ANOVA (two-way repeated measures ANOVA) followed by *post hoc* Dunnett test. Multiple comparisons were analyzed by one-way ANOVA and *post hoc* Tukey test. There were no missing data. For the mechanical hyperalgesia testing no statistical power calculation was conducted before the study. The sample size was based on our previous experience with this design. For the biochemical and immunohistochemical experiments that were done in duplicate or triplicate a minimum number of five independent animals were used. Statistical significance was assumed at $P < 0.05$.

Results

Mineralocorticoid Receptor Antagonism Results in Rapid, Nongenomic and Short-lasting Reduction of Inflammation-induced Mechanical Hypersensitivity

Four days of Freund's complete adjuvant–induced inflammation of the right hind paw resulted in significantly reduced mechanical paw pressure thresholds of the inflamed but not the contralateral noninflamed hind paws compared to baseline values ($P < 0.001$; independent paired Student *t* test; fig. 1). This enhanced mechanical hypersensitivity was dose-dependent and rapidly reversed after systemic administration of the mineralocorticoid receptor selective antagonist canrenoate-K ($P < 0.001$; two-way repeated measures ANOVA, *post hoc* Dunnett test; fig. 1A). Intrathecal application of lower doses of canrenoate-K also resulted in rapid and transient attenuation of the Freund's complete adjuvant inflammation–induced mechanical hypersensitivity ($P < 0.001$; two-way ANOVA, *post hoc* Dunnett test; fig. 1B). Intrathecal canrenoate-K had no effect on the contralateral noninflamed hind paws (data not shown), similar to previous reports in naive rats.[19]

Coexpression of Mineralocorticoid Receptors with Its Protecting Enzyme 11β-Hydroxysteroid-Dehydrogenase 2 in Sensory Dorsal Root Ganglia

Since, it is well established that the mineralocorticoid receptor protecting enzyme 11β-hydroxysteroid-dehydrogenase 2[30] immediately converts corticosterone to its inactive metabolite 11-dehydrocorticosterone and ensures mineralocorticoid receptor activation only through endogenous aldosterone, we have examined the coexpression of mineralocorticoid receptors with 11β-hydroxysteroid-dehydrogenase 2 in sensory dorsal root ganglia. TaqMan quantitative polymerase chain reaction (fig. 2, A and B) and western blot (fig. 2, C and D) analysis identified 11β-hydroxysteroid-dehydrogenase 2 specific mRNA and 11β-hydroxysteroid-dehydrogenase 2 specific protein bands (70 kDa) in dorsal root ganglia. Moreover, double immunofluorescence confocal microscopy showed that 11β-hydroxysteroid-dehydrogenase 2 immunoreactivity mainly colocalized with mineralocorticoid receptor–immunoreactive sensory neurons which further increased in dorsal root ganglia ipsilateral to Freund's complete adjuvant–inflamed hind paws compared to controls ($P < 0.001$; two-tailed independent Student *t* test; fig. 2, E to M). In parallel, 11β-hydroxysteroid-dehydrogenase 2-immunoreactive dorsal root ganglia cells predominantly colocalized with the peptidergic sensory neuron marker calcitonin-gene-related peptide but only scarcely with some satellite cell-like structures confirming our previous study; 11β-hydroxysteroid-dehydrogenase 2-immunoreactive dorsal root ganglia cells colocalized with calcitonin-gene-related peptide in 58 ± 12% of control animals and in 62 ± 17% of rats with hind paw inflammation ($P = 0.619$; two-tailed independent Student *t* test; Supplemental Digital Content, fig. S1, http://links.lww.com/ALN/C235).

Inflammation-dependent Increase of Endogenous Aldosterone Primarily in Mineralocorticoid- and Calcitonin Gene–Related Peptide Immunoreactive Sensory Dorsal Root Ganglia, But Not in Plasma

The selective mineralocorticoid receptor antagonist, canrenoate-K, reversed Freund's complete adjuvant–induced mechanical hypersensitivity suggesting intrinsic mineralocorticoid receptor activation by endogenous aldosterone, therefore, we investigated whether aldosterone could be identified in dorsal root ganglia. Double immunofluorescence confocal microscopy showed abundant colocalization of aldosterone with mineralocorticoid receptors (fig. 3, A to F), as well as aldosterone with the sensory neuron marker calcitonin gene–related peptide (fig. 3, J to O) in control animals. Aldosterone—together with either mineralocorticoid receptor (fig. 3, G and I—or calcitonin gene–related peptide immunoreactive dorsal root ganglia

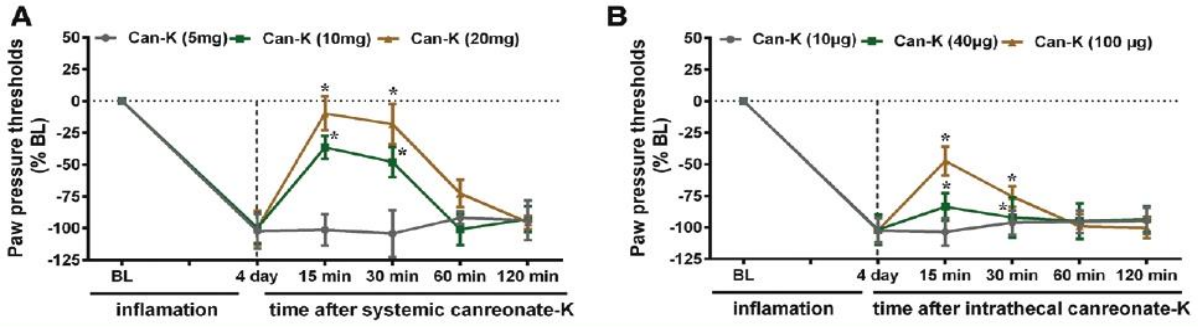

Fig. 1. Role of mineralocorticoid receptor specific antagonist canrenoate-K (Can-K) in the modulation of inflammation-induced nociceptive behavior in the right hind paw. (*A, B*) Four days of Freund's complete adjuvant–induced inflammation of the right hind paw resulted in significantly reduced mechanical paw pressure thresholds (shown as % BL, *i.e.*, % baseline values) compared to baseline values (*dotted horizontal line*; $P < 0.001$; independent paired Student *t* test; n = 7 [*A*], 8 [*B*] rats; experiments in triplicate). Increasing doses of systemic (*A*) or intrathecal (*B*) canrenoate-K reversed this mechanical hypersensitivity within minutes ($P < 0.001$; two-way repeated measures ANOVA, *post hoc* Dunnett test; n = 7 [*A*], 8 [*B*] rats; experiments in triplicate). Can-K shows a transient attenuation of the endogenous tonic activation of mineralocorticoid receptors during hind paw inflammation. Data are expressed as mean ± SD. BL, baseline.

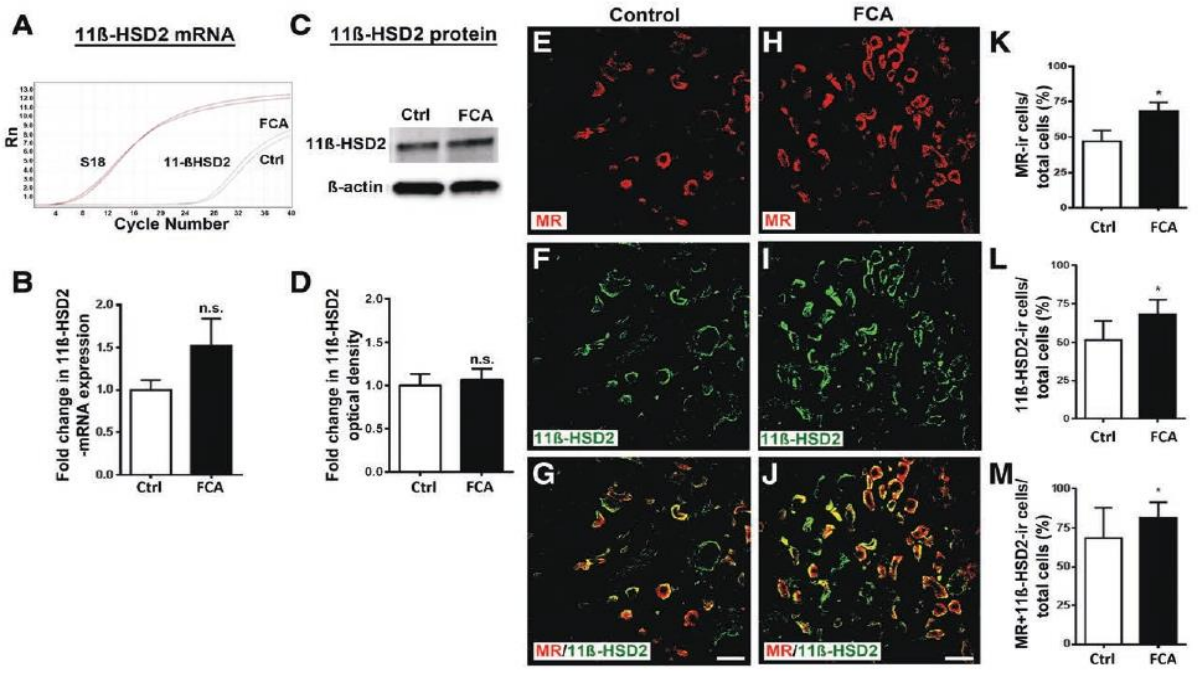

Fig. 2. Detection of 11ß-hydroxysteroid dehydrogenase type 2 (11ß-HSD2) mRNA and protein in dorsal root ganglia of FCA-treated rats compared to controls (Ctrl). (*A* to *D*) Quantification of 11ß-HSD2 mRNA (*A, B*) using TaqMan quantitative polymerase chain reaction and Western blot (*C, D*) shows a significant increase in 11ß-HSD2 mRNA (*A, B*), but not protein (*C, D*) in dorsal root ganglia of FCA treated rats compared to controls ($P < 0.001$; two-tailed independent Student *t* test; n = 5 rats; experiments in triplicate for TaqMan polymerase chain reaction and in duplicate for Western blot). (*E* to *J*) Confocal microscopy of double immunofluorescence of 11ß-HSD2 (*green fluorescence*) with MR (*red fluorescence*) in dorsal root ganglia of FCA treated rats *versus* controls (*K* to *M*). Note that the majority of 11ß-HSD2 immunoreactivity colocalized (*L*) with MR-immunoreactive neurons and significantly increased in FCA treated rats compared to controls (*M*; $P < 0.001$; two-tailed independent Student *t* test; n = 5 rats; 3-4 tissue sections each; *K*). Bar = 40 µm. Data are expressed as mean ± SD. FCA, Freund's complete adjuvant; IR, immunoreactive; MR, mineralocorticoid receptor.

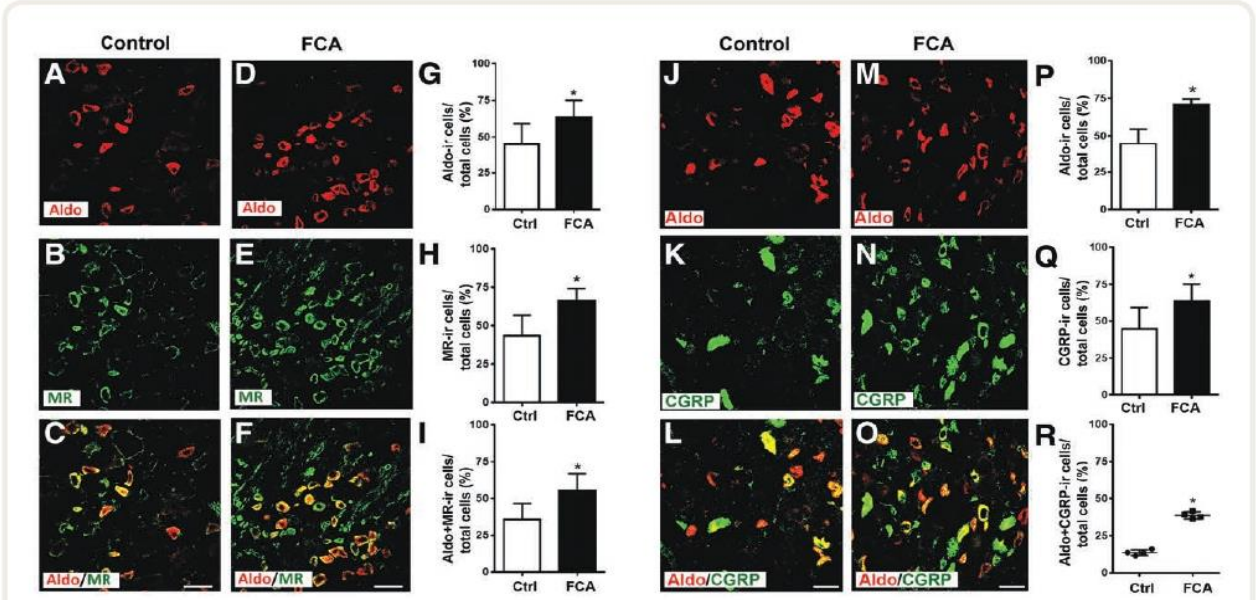

Fig. 3. Detection of aldosterone with MR (*A* to *I*) or CGRP (*J* to *R*) in dorsal root ganglia of FCA-treated rats *versus* controls. (*A* to *F, J* to *O*) Double immunofluorescence confocal microscopy of aldosterone (*red fluorescence)* with MR (*A* to *I*) or CGRP (*J* to *R*) (*green fluorescence)* in dorsal root ganglia sections (Bar = 40 μm). The number of Aldo- (*G, P*), MR- (*H, I*) or CGRP- (*Q, R*) immunoreactive neurons in relation to the total number of dorsal root ganglia neurons was significantly increased in FCA treated rats compared to controls ($P < 0.001$; two-tailed independent Student *t* test). In addition, the colocalization of Aldo with MR (*C, F, I*) or CGRP (*M, O, R*) in dorsal root ganglia neurons was significantly increased in FCA animals (*I, R*; $P < 0.001$; two-tailed independent Student *t* test; n = 4, 5 rats; 3-4 tissue sections each). Bar = 40 μm. Data are expressed as mean ± SD. Aldo, aldosterone; CGRP, calcitonin gene–related peptide; Ctrl, controls; FCA, Freund's complete adjuvant; IR, immunoreactive; MR, mineralocorticoid receptors.

increased significantly (fig. 3, P to R) following Freund's complete adjuvant hind paw inflammation ($P < 0.001$; two-tailed independent Student *t* test; fig. 3).

Using a highly specific aldosterone ELISA, we identified immunoreactive aldosterone in dorsal root ganglia of naïve control animals (2.8 ± 0.7 pg/mg) and demonstrated its significant upregulation after 4 days of Freund's complete adjuvant–inflammation (7.4 ± 1.2 pg/mg; $P < 0.01$; two-tailed independent Student *t* test; fig. 4A). In contrast, aldosterone plasma concentrations in Freund's complete adjuvant–treated rats *versus* controls were not significantly altered ($P = 0.353$; two-tailed independent Student *t* test; fig. 4B).

Aldosterone Synthase mRNA and Protein Expression in Aldosterone- and Mineralocorticoid Receptor–Immunoreactive Dorsal Root Ganglia

Since aldosterone is derived from a final conversion of 18-hydroxycorticosterone into aldosterone by aldosterone synthase, we examined the local expression of this enzyme in sensory dorsal root ganglia. Quantitative TaqMan assay using mRNA specific primers detected aldosterone synthase mRNA in dorsal root ganglia which significantly increased following Freund's complete adjuvant hind paw inflammation ($P < 0.01$; two-tailed independent Student *t* test; fig. 4, C and D). Furthermore, these observations were supported by the identification of aldosterone synthase specific protein bands (57 kDa) in sensory dorsal root ganglia and their increase after hind paw inflammation (fig. 4, E and F). In addition, double immunofluorescence confocal microscopy showed coexistence of aldosterone with its key processing enzyme in neuronal structures of dorsal root ganglia of inflamed and control rats (fig. 5). Moreover, aldosterone synthase colocalized with mineralocorticoid receptor–immunoreactive neurons that further increased following hind paw inflammation ($P = 0.01$; two-tailed independent Student *t* test; fig. 5, G to I, P to R).

Physical Link between Endogenous Aldosterone and Membrane-bound Mineralocorticoid Receptors in Sensory Dorsal Root Ganglia

Immunoprecipitation of whole protein extracts of dorsal root ganglia membrane fractions with anti-aldosterone antibody pulls down multiple proteins that are complexed with aldosterone. Subsequent Western blot analysis of these functional complex formations resulted in the identification of proteins coprecipitated with aldosterone, such as

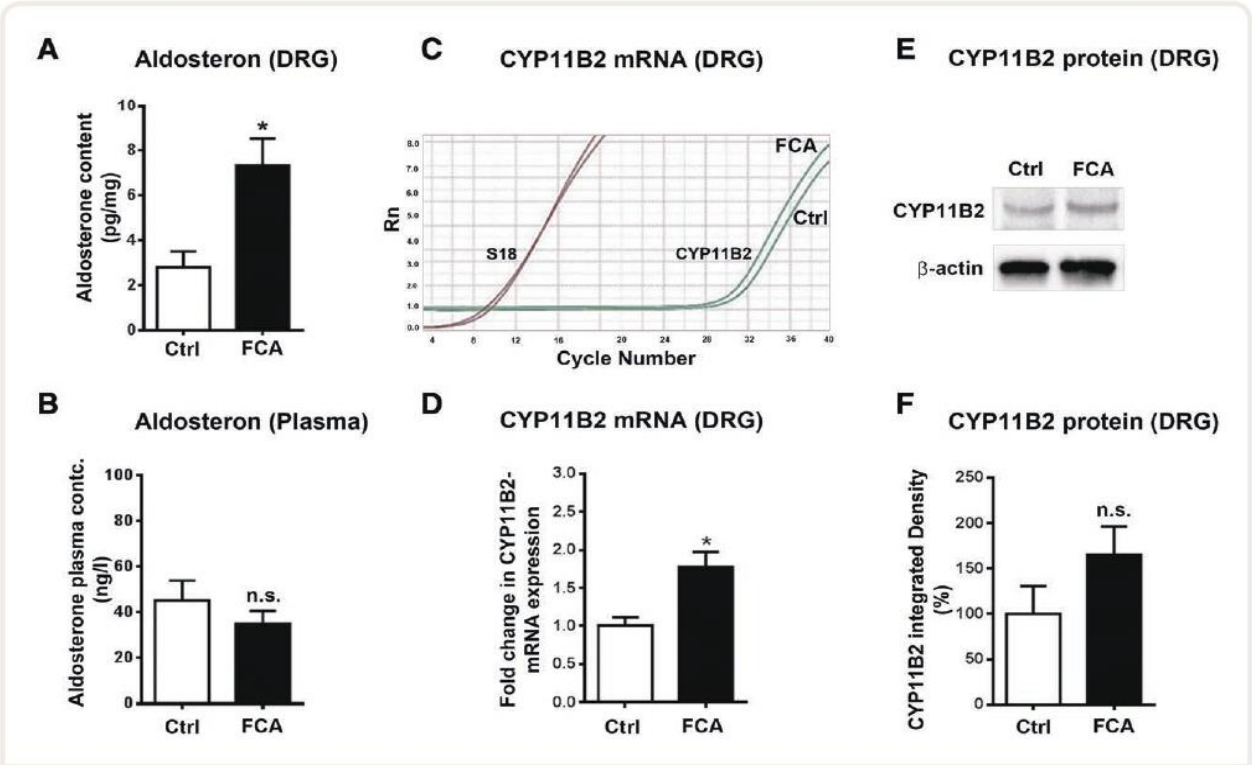

Fig. 4. Detection of aldosterone, as well as its processing enzyme aldosterone synthase, CYP11B2 mRNA, and protein in dorsal root ganglia (DRG) of Freund's complete adjuvant (FCA)–treated rats compared to controls (Ctrl). (*A*) Using an aldosterone specific enzyme-linked immunosorbent assay kit a significant increase in aldosterone content was shown in DRG of FCA-treated rats compared to controls ($P < 0.01$; two-tailed independent Student *t* test; n = 5, 6 rats; experiments in triplicate). (*B*) However, aldosterone plasma concentrations showed no significant differences ($P = 0.353$; two-tailed independent Student *t* test; blood from n = 15, 17 rats). (*C* to *F*) Quantification of aldosterone synthase CYP11B2 mRNA using TaqMan quantitative polymerase chain reaction (*C, D*) and protein using western blot (*E, F*) revealed a significant increase in CYP11B2 mRNA (*D*; $P = 0.043$), but not in protein (*F*; $P = 0.189$) in DRG of FCA-treated rats compared to Ctrl (two-tailed independent Student *t* test; n = 5; experiments in triplicate for TaqMan quantitative polymerase chain reaction and in duplicate for Western blot). Data are expressed as mean ± SD. n.s., nonsignificant differences.

membranous mineralocorticoid receptor and the transmembrane molecule ß1-integrin (fig. 6). Interestingly, the coprecipitated mineralocorticoid receptor protein band showed a higher optical density in dorsal root ganglia innervating inflamed hind paws than in control normal dorsal root ganglia (fig. 6). ß-actin protein bands were not detectable in the membrane fraction but in the cytosolic lysate.

Intrathecal Aldosterone Synthase Inhibitor FAD286 Reduces Aldosterone Content in Dorsal Root Ganglia and Attenuates Inflammatory Mechanical Hypersensitivity

Since endogenous aldosterone content was significantly increased in sensory dorsal root ganglia after inflammation, we examined whether intrathecal infusion of aldosterone synthase inhibitor FAD286 abolished this increase. Indeed, our confocal immunofluorescence analysis showed that intrathecal infusion of FAD286, but not the vehicle, significantly reduced the number of aldosterone-immunoreactive dorsal root ganglia in relation to the total number of dorsal root ganglion cells in Freund's complete adjuvant–treated rats ($P < 0.001$; one-way ANOVA and *post hoc* Dunnett test; fig. 7, A to D). Moreover, our aldosterone-specific ELISA revealed that the increase in aldosterone content in dorsal root ganglia of Freund's complete adjuvant–treated animals was significantly reduced by intrathecal treatment with aldosterone synthase inhibitor FAD286 ($P < 0.001$; one-way ANOVA and *post hoc* Dunnett test; fig. 7E). Consistent with the reduction of aldosterone content in sensory dorsal root ganglia, the enhanced mechanical hypersensitivity was significantly diminished following intrathecal aldosterone inhibitor FAD286 ($P < 0.001$; one-way ANOVA and *post hoc* Dunnett test; fig. 7F).

Discussion

The main findings of this investigation are: (1) blocking an ongoing intrinsic tone of mineralocorticoid receptor activation

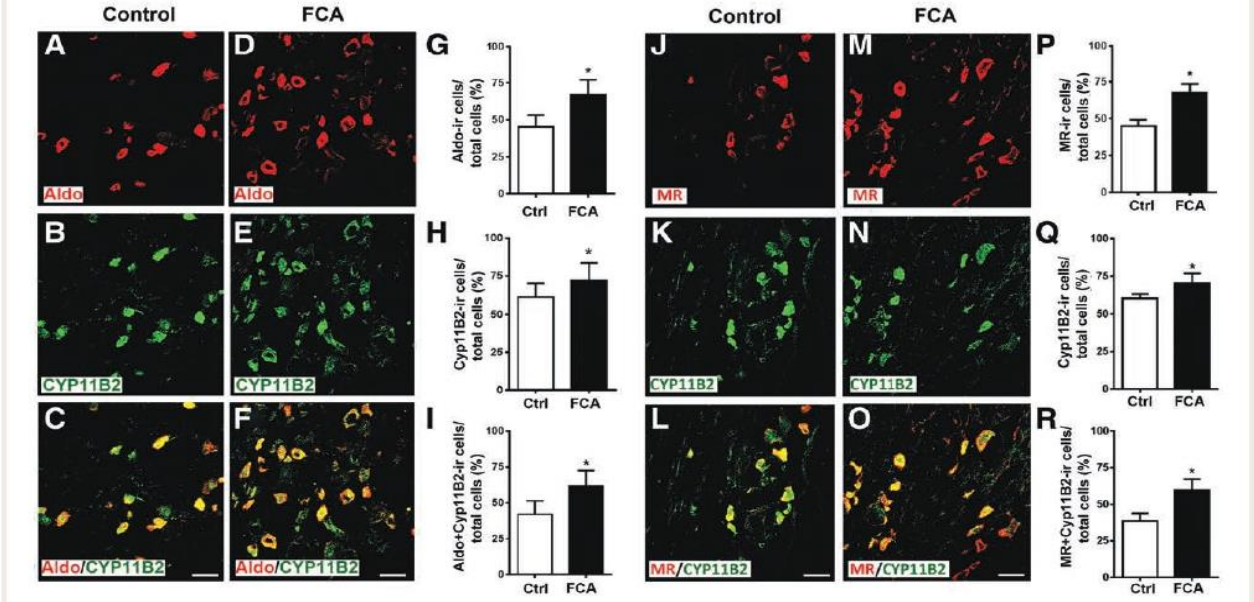

Fig. 5. Detection of aldosterone synthase CYP11B2 with aldosterone (Aldo) and mineralocorticoid receptor (MR) in dorsal root ganglia of Freund's complete adjuvant (FCA)–treated rats *versus* controls (Ctrl). (*A, E*) Confocal microscopy of double immunofluorescence of CYP11B2 (*green fluorescence*) with Aldo (*A* to *I*) or MR (*J* to *R*) (*red fluorescence*) in dorsal root ganglia of FCA-treated rats *versus* controls. Note that the majority of CYP11B2 immunoreactivity colocalized with Aldo- (*C, F, I*) or MR- (*L, O, R*) immunoreactive (IR) neurons. The number of Aldo- (*G*), MR- (*P*), or CYP11B2- (*H, Q*) IR neurons in relation to the total number of dorsal root ganglia neurons was significantly increased in FCA-treated rats compared to controls ($P < 0.001$, two-tailed independent Student *t* test). In addition, the colocalization of aldosterone (*I*) or MR (*R*) with CYP11B2 in dorsal root ganglia neurons was significantly increased in FCA animals ($P < 0.01$; two-tailed independent Student *t* test; n = 5 rats; experiments in triplicate). Bar = 40 µm. Data are expressed as mean ± SD.

in sensory dorsal root ganglia during hind paw inflammation inhibits nociceptive mechanical hypersensitivity; (2) the identification of endogenous aldosterone with its processing enzyme aldosterone synthase in sensory dorsal root ganglia indicates local aldosterone production; (3) the upregulation of aldosterone synthase mRNA and protein is concomitant with an enhanced aldosterone content in sensory dorsal root ganglia after hind paw inflammation; (4) the demonstration of a physical link between the endogenous ligand aldosterone and mineralocorticoid receptor in sensory dorsal root ganglia; and (5) the inhibition of the aldosterone synthase enzyme in sensory dorsal root ganglia attenuates inflammation-induced mechanical hypersensitivity. Overall, these findings suggest that the local production of aldosterone within peripheral sensory dorsal root ganglia contributes to ongoing nociceptive mechanical hypersensitivity *via* intrinsic activation of neuronal mineralocorticoid receptors. Thus, aldosterone synthase (*i.e.*, aldosterone-converting enzyme CYP11B2) represents a novel target for the potential modulation of nociceptive mechanical hypersensitivity during inflammation.

In our animal model of persistent inflammation-induced mechanical hyperalgesia in the right hind paw, the systemic, as well as intrathecal administration of the mineralocorticoid receptor antagonist, canrenoate-K, resulted in rapid (within minutes), short-lasting (30 to 60 min), and transient inhibition of mechanical hyperalgesia. This inhibition of mechanical hyperalgesia most likely indicates a rapid nongenomic effect based on the temporary antagonism of mineralocorticoid receptors on peripheral sensory dorsal root ganglia,[16,22] resulting in the inhibition of intrinsic tonic mineralocorticoid receptor activation by an endogenous ligand that apparently contributes to mechanical hyperalgesia. Our current findings are in line with previous studies reporting the antinociceptive effects of the mineralocorticoid receptor antagonist eplerenone[2,15,17] or spironolactone.[13,14] However, these effects were observed only after 3 days and lasted up to 2 weeks suggesting a slowly developing, but long-lasting genomic effect.

Mineralocorticoid receptors are located mainly on the peptidergic (calcitonin gene–related peptide immunoreactive) subpopulation of peripheral nociceptive neurons.[22] Moreover, previous studies suggested that the endogenous ligand aldosterone facilitates action potentials in dorsal root ganglion neurons[2,15] and elicits mechanical hypersensitivity in naïve animals.[22] Li *et al.*[19] consistently showed that the antagonism of mineralocorticoid receptors attenuates inflammation-induced nociceptive

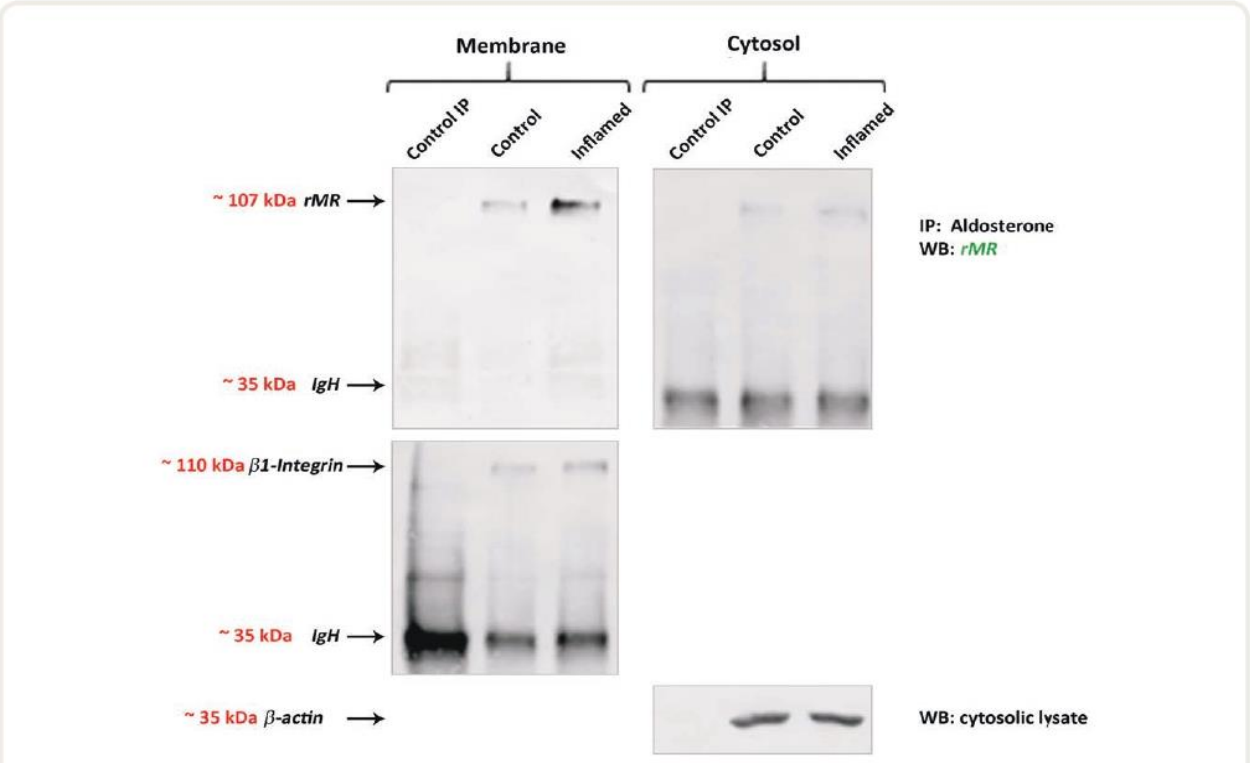

Fig. 6. Immunoprecipitation of whole protein extracts of dorsal root ganglia membrane and cytosol fractions with anti-aldosterone antibody and subsequent Western blot in dorsal root ganglia of rats with hind paw inflammation *versus* controls. L4–L5 dorsal root ganglia membrane and cytosol fraction extracts were lysed and immunoprecipitated with anti-aldosterone and subsequently the immunoprecipitants were separated by sodium dodecyl sulfate–polyacrylamide gel electrophoresis and analyzed by immunoblotting using anti–mineralocorticoid receptor and anti-ß1 integrin antibody. The ß-actin blot is shown only for the cytosolic lysate because ß-actin cannot be found in the membrane fraction. IgH, immunoglobulin heavy chain; IP, immunoprecipitation; rMR, mineralocorticoid receptor; WB, Western blot.

behavior by nongenomic mechanisms. Mineralocorticoid receptors in kidney tissue[31] and other peripheral tissues[32] are protected by the enzyme 11β-hydroxysteroid-dehydrogenase 2 from inadvertent activation by corticosterone through its conversion into inactive 11-dehydrocorticosterone.[33] Earlier reports have suggested that 11β-hydroxysteroid-dehydrogenase 2 functions as a gate keeper[33] and ensures mineralocorticoid receptor occupancy only by mineralocorticoids.[32] Interestingly, the current study identified 11β-hydroxysteroid-dehydrogenase 2 specific mRNA and protein in dorsal root ganglia and demonstrated its colocalization with calcitonin gene–related peptide, a marker specific for peptidergic nociceptive dorsal root ganglion neurons. Moreover, we found an approximately 80% coexistence of mineralocorticoid receptors with 11β-hydroxysteroid-dehydrogenase 2-immunoreactive neurons. Taken together these observations imply ongoing intrinsic mineralocorticoid receptor activation is due to endogenous aldosterone.

Recent emerging evidence suggests that extra-adrenal synthesis of aldosterone occurs and has local paracrine effects within the heart[5,7] and brain.[9–11,30] In the current study, the double immunofluorescence confocal microscopy showed abundant aldosterone immunoreactivity in dorsal root ganglion neurons which strongly colocalized with the sensory neuron marker calcitonin gene–related peptide and its corresponding receptor (*i.e.,* the mineralocorticoid receptor). These findings are in agreement with previous reports that suggested a putative paracrine mechanism of aldosterone in contributing to cardiac fibrosis.[34] Several investigators have postulated that the aldosterone may be synthesized in neurons located within the hypothalamus and the rostral ventral medulla of the brain appeared to contribute to their depolarization.[9–11,30] For further support of the local production of aldosterone within the neuron, the current experiments observed that aldosterone-immunoreactive dorsal root ganglion neurons coexpressed to a high degree (90%) the aldosterone synthase which is responsible for the conversion from 18-hydroxycorticosterone to active aldosterone.[9] This is in line with previous studies in hippocampal neurons in which the aldosterone producing enzymes 11ß-hydroxylase

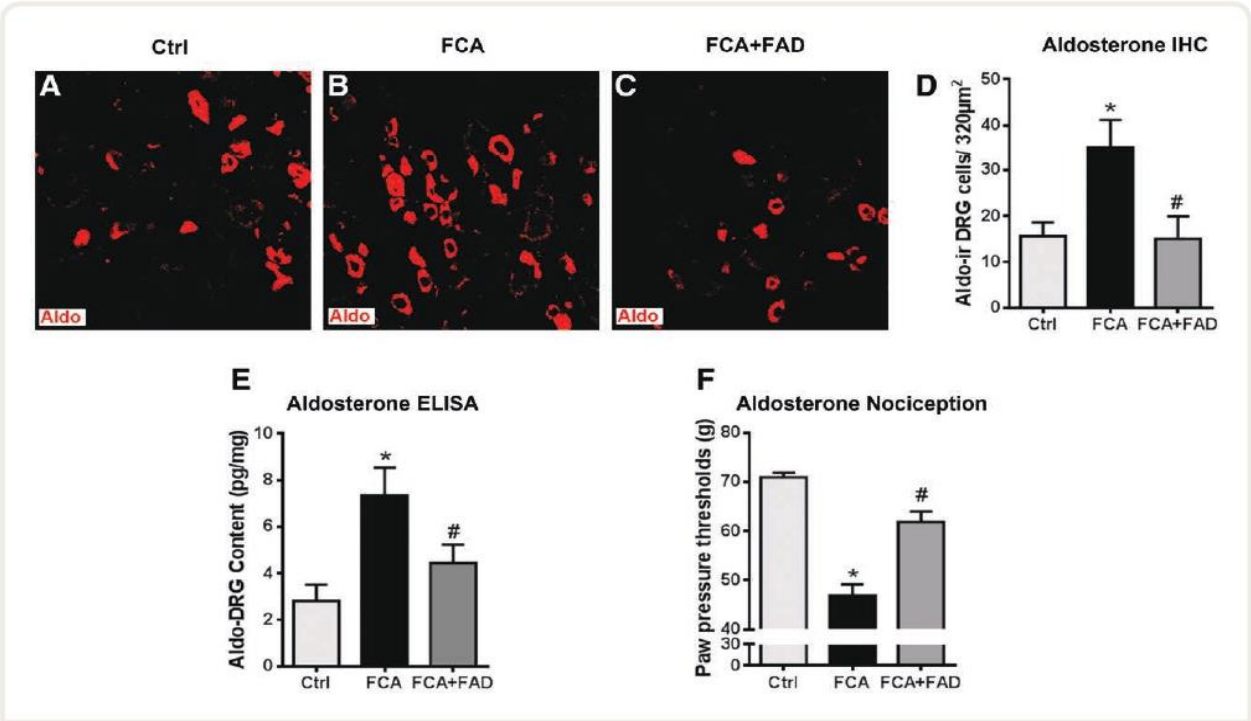

Fig. 7. Impact of aldosterone synthase inhibitor FAD286 on Freund's complete adjuvant (FCA) inflammation–induced aldosterone upregulation in dorsal root ganglia (DRG) (*A* to *E*) and on nociceptive behavior (*F*). (*A* to *D*) Determination of aldosterone-immunoreactive DRG neurons of FCA rats treated with it aldosterone synthase inhibitor FAD286. Note, the number of aldosterone-immunoreactive DRG neurons in FCA rats was increased by approximately 2.2-fold compared to controls which reversed after continuous intrathecal aldosterone synthase inhibitor FAD286 treatment for more than 5 days ($P < 0.001$; two-tailed independent Student *t* test; n = 5 rats, 3 to 4 tissue sections each). (*E*) Determination of aldosterone content in dorsal root ganglia of FCA rats treated with it aldosterone synthase inhibitor FAD286 by a fluorometric enzyme–linked immunoassay. Note, Aldo content in DRG of FCA rats increased by approximately 2.6-fold compared to control which was reversed after intrathecal aldosterone synthase inhibitor FAD286 treatment ($P < 0.001$; two-tailed independent Student *t* test; n = 5, 6, 6 rats; experiments in triplicate). (*F*) Intrathecal FAD286 resulted in significant mechanical paw pressure threshold elevations compared to baseline (0 min), indicating a reversal of FCA inflammation–induced mechanical hyperalgesia ($P < 0.001$; one-way repeated measures ANOVA, followed by *post hoc* Dunnett test; n = 7, 7, 10 rats; experiments in triplicate). Aldo, aldosterone; ELISA, enzyme-linked immunosorbent assay; FAD, FAD286; IHC, immunohistochemistry; IR, immunoreactive.

and aldosterone synthase were identified by reverse transcriptase polymerase chain reaction and immunostaining.[12,35,36] In our animal model of local inflammation, both aldosterone synthase mRNA transcripts and specific protein bands were significantly upregulated in dorsal root ganglia compared to controls. Consistently, both the number of aldosterone-immunoreactive dorsal root ganglion neurons and the aldosterone content of dorsal root ganglia significantly increased under inflammatory conditions, while aldosterone plasma concentrations remained unchanged. Therefore, our findings suggest an enhanced expression of aldosterone-producing enzyme, aldosterone synthase, and subsequent accumulation of converted aldosterone in dorsal root ganglia, which points toward an enhanced intrinsic tone of endogenous aldosterone. Furthermore, immunoprecipitation of dorsal root ganglia membrane fractions with aldosterone antibody followed by anti–mineralocorticoid receptor immunoblotting showed the coprecipitation of functional complex formations of endogenous aldosterone with membrane-bound mineralocorticoid receptors, suggesting a physical link. Our data, showing membrane-bound mineralocorticoid receptors, is supported by electron microscopy studies in presynaptic terminals and postsynaptic densities within certain brain areas.[37,38]

Since aldosterone content in peripheral sensory dorsal root ganglia was significantly increased following inflammation, we examined whether intrathecal infusion of a specific aldosterone synthase inhibitor reestablished baseline aldosterone concentrations in dorsal root ganglia of control animals. Indeed, consistent with aldosterone synthase inhibition within neurons of the brain,[10,11,18] continuous intrathecal infusion of the aldosterone inhibitor FAD286 during 4 days significantly reduced dorsal root ganglion aldosterone content, as well as the number of aldosterone-immunoreactive dorsal root ganglion neurons in Freund's complete adjuvant–treated

rats. Consequently, our behavioral experiments showed that the enhanced mechanical hypersensitivity associated with inflamed hind paws was inhibited after intrathecal aldosterone synthase inhibition. Therefore, our observations showed for the first time that the peripheral sensory dorsal root ganglia are the main site for local synthesis of active aldosterone, which contribute to ongoing mechanical hypersensitivity *via* intrinsic activation of neuronal mineralocorticoid receptors.

Limitations of the study are that demonstration of mineralocorticoid receptors, aldosterone, and aldosterone synthase mRNA by TaqMan quantitative polymerase chain reaction and respective proteins by Western blot in dorsal root ganglia do not necessarily demonstrate their expression in peripheral sensory neurons because dorsal root ganglia not only contain cell bodies of sensory neurons, but also satellite glial cells, fibroblasts, and sparse immune cells. However, our immunohistochemical staining clearly shows that the majority of cells expressing mineralocorticoid receptors, aldosterone, and the processing enzyme aldosterone synthase in dorsal root ganglia are sensory neurons. In addition, evidence for dorsal root ganglia–derived aldosterone has been convincingly demonstrated by different methods (*e.g.,* TaqMan quantitative polymerase chain reaction, Western blot, immunohistochemistry, ELISA, and inhibition of the processing enzyme aldosterone synthase) has shown a reduction in dorsal root ganglia–derived aldosterone with subsequent attenuation of inflammation-induced mechanical hypersensitivity. Differences between the semiquantitative Western blot results and the immunohistochemical counting of immunoreactive cells for the same protein (*e.g.*, 11β-hydroxysteroid-dehydrogenase 2; fig. 2, C and L) might be due to the differences in the assay sensitivity. Another limitation is the relatively small sample size of animals per group and the restriction to male rats, so that the observed significant differences may have occurred by pure chance and may not be detected in female rats. Further limitation might come from the lack of randomization which does not exclude a systematic error due to potential differences among animals even if animals are recruited from an inbred strain.

In summary, our data show that the selective mineralocorticoid receptor antagonist, canrenoate-K, rapidly inhibits mechanical hypersensitivity during inflammatory conditions, suggesting a tonic activation of mineralocorticoid receptors by an endogenous ligand. Indeed, aldosterone synthase mRNA and protein were significantly increased concomitant with enhanced aldosterone content in mineralocorticoid receptor–immunoreactive sensory neurons following local inflammation. Importantly, inhibition of the aldosterone synthase in sensory dorsal root ganglia significantly reduced aldosterone content and consequently attenuated inflammation-induced mechanical hypersensitivity. These findings provide the first evidence that the local production of aldosterone *via* aldosterone synthase within peripheral sensory dorsal root ganglia contributes to ongoing mechanical hypersensitivity *via* intrinsic activation of neuronal mineralocorticoid receptors (Supplemental Digital Content, fig. S2, http://links.lww.com/ALN/C235). This novel concept needs further validation studies in order to be translated eventually into humans.

Acknowledgments

The authors thank Mrs. Petra von Kwiatkowski (Technician, Berlin, Germany) for her technical assistance. The authors are very grateful for the gift of the glucocorticoid receptor and mineralocorticoid receptor antibodies from Drs. M. Kawata (Department of Anatomy and Neurobiology, Kyoto Prefectural University of Medicine, Kyoto, Japan) and E. Gomez-Sanchez (Montgomery Veteran's Affairs Medical Center, Jackson, Mississippi). The incentive of this work has been given the earlier clinical findings of the beneficial role of corticosteroid receptor agonists/antagonists in patients with inflammation and pain by Prof. K. H. René Koczorek (Department of Medicine, Ludwig-Maximilians-Universität München, München, Germany).

Research Support

Supported by the Prof. K. H. René Koczorek Foundation (Neuried, Germany). Doaa M. Mohamed was supported by a scholarship from the Faculty of Science at Aswan University (Aswan, Egypt) and the Egyptian government.

Competing Interests

The authors declare no competing interests.

Correspondence

Address correspondence to Dr. Mousa: Department of Anesthesiology and Intensive Care Medicine, Charité University Berlin, Campus Benjamin Franklin, Hindenburgamm 30, 12203 Berlin, Germany. shaaban.mousa@charite.de.

References

1. Cole TJ, Young MJ: 30 Years of the mineralcorticoid receptor: Mineralocorticoid receptor null mice: Informing cell-type-specific roles. J Endocrinol 2017; 234:T83–92
2. Schumacher MA: Back pain and the mineralocorticoid receptor: Is there a connection? ANESTHESIOLOGY 2012; 117:951–2
3. Gardner DG, Shoback DM: Greenspan's Basic and Clinical Endocrinology. United Kingdom, McGraw-Hill Education, 2017, p 10
4. Lockett MF, Retallack RW: The influence of heart rate on the secretion of a substance closely resembling the 18-monoacetate of D-aldosterone by the hearts of cats under chloralose anaesthesia. J Physiol 1970; 208:21–32

5. Silvestre JS, Robert V, Heymes C, Aupetit-Faisant B, Mouas C, Moalic JM, Swynghedauw B, Delcayre C: Myocardial production of aldosterone and corticosterone in the rat. Physiological regulation. J Biol Chem 1998; 273:4883–91
6. Takeda R, Hatakeyama H, Takeda Y, Iki K, Miyamori I, Sheng WP, Yamamoto H, Blair IA: Aldosterone biosynthesis and action in vascular cells. Steroids 1995; 60:120–4
7. Mizuno Y, Yoshimura M, Yasue H, Sakamoto T, Ogawa H, Kugiyama K, Harada E, Nakayama M, Nakamura S, Ito T, Shimasaki Y, Saito Y, Nakao K: Aldosterone production is activated in failing ventricle in humans. Circulation 2001; 103:72–7
8. Yoshimura M, Nakamura S, Ito T, Nakayama M, Harada E, Mizuno Y, Sakamoto T, Yamamuro M, Saito Y, Nakao K, Yasue H, Ogawa H: Expression of aldosterone synthase gene in failing human heart: Quantitative analysis using modified real-time polymerase chain reaction. J Clin Endocrinol Metab 2002; 87:3936–40
9. Colombo L, Dalla Valle L, Fiore C, Armanini D, Belvedere P: Aldosterone and the conquest of land. J Endocrinol Invest 2006; 29:373–9
10. Oshima N, Onimaru H, Takechi H, Yamamoto K, Watanabe A, Uchida T, Nishida Y, Oda T, Kumagai H: Aldosterone is synthesized in and activates bulbospinal neurons through mineralocorticoid receptors and ENaCs in the RVLM. Hypertens Res 2013; 36:504–12
11. Wang HW, Huang BS, White RA, Chen A, Ahmad M, Leenen FH: Mineralocorticoid and angiotensin II type 1 receptors in the subfornical organ mediate angiotensin II - induced hypothalamic reactive oxygen species and hypertension. Neuroscience 2016; 329:112–21
12. MacKenzie SM, Connell JM, Davies E: Non-adrenal synthesis of aldosterone: A reality check. Mol Cell Endocrinol 2012; 350:163–7
13. Gu X, Peng L, Yang D, Ma Q, Zheng Y, Liu C, Zhu B, Song L, Sun X, Ma Z: The respective and interaction effects of spinal GRs and MRs on radicular pain induced by chronic compression of the dorsal root ganglion in the rat. Brain Res 2011; 1396:88–95
14. Sun YE, Peng L, Sun X, Bo J, Yang D, Zheng Y, Liu C, Zhu B, Ma Z, Gu X: Intrathecal injection of spironolactone attenuates radicular pain by inhibition of spinal microglia activation in a rat model. PLoS One 2012; 7:e39897
15. Dong F, Xie W, Strong JA, Zhang JM: Mineralocorticoid receptor blocker eplerenone reduces pain behaviors *in vivo* and decreases excitability in small-diameter sensory neurons from local inflamed dorsal root ganglia *in vitro*. Anesthesiology 2012; 117:1102–12
16. Shaqura M, Li X, Al-Madol MA, Tafelski S, Beyer-Koczorek A, Mousa SA, Schäfer M: Acute mechanical sensitization of peripheral nociceptors by aldosterone through non-genomic activation of membrane bound mineralocorticoid receptors in naive rats. Neuropharmacology 2016; 107:251–61
17. Ye L, Xie W, Strong JA, Zhang JM: Blocking the mineralocorticoid receptor improves effectiveness of steroid treatment for low back pain in rats. Anesthesiology 2014; 121:632–43
18. Deliyanti D, Miller AG, Tan G, Binger KJ, Samson AL, Wilkinson-Berka JL: Neovascularization is attenuated with aldosterone synthase inhibition in rats with retinopathy. Hypertension 2012; 59:607–13
19. Li X, Shaqura M, Mohamed D, Beyer A, Yamada S, Mousa SA, Schäfer M: Pro- *versus* antinociceptive nongenomic effects of neuronal mineralocorticoid *versus* glucocorticoid receptors during rat hind paw inflammation. Anesthesiology 2018; 128:796–809
20. Rittner HL, Brack A, Machelska H, Mousa SA, Bauer M, Schäfer M, Stein C: Opioid peptide-expressing leukocytes: Identification, recruitment, and simultaneously increasing inhibition of inflammatory pain. Anesthesiology 2001; 95:500–8
21. Shaqura M, Khalefa BI, Shakibaei M, Winkler J, Al-Khrasani M, Fürst S, Mousa SA, Schäfer M: Reduced number, G protein coupling, and antinociceptive efficacy of spinal mu-opioid receptors in diabetic rats are reversed by nerve growth factor. J Pain 2013; 14:720–30
22. Shaqura M, Li X, Al-Khrasani M, Shakibaei M, Tafelski S, Fürst S, Beyer A, Kawata M, Schäfer M, Mousa SA: Membrane-bound glucocorticoid receptors on distinct nociceptive neurons as potential targets for pain control through rapid non-genomic effects. Neuropharmacology 2016; 111:1–13
23. Mousa SA, Shaqura M, Khalefa BI, Zöllner C, Schaad L, Schneider J, Shippenberg TS, Richter JF, Hellweg R, Shakibaei M, Schäfer M: Rab7 silencing prevents μ-opioid receptor lysosomal targeting and rescues opioid responsiveness to strengthen diabetic neuropathic pain therapy. Diabetes 2013; 62:1308–19
24. Mousa SA, Shaqura M, Winkler J, Khalefa BI, Al-Madol MA, Shakibaei M, Schulz S, Schäfer M: Protein kinase C-mediated mu-opioid receptor phosphorylation and desensitization in rats, and its prevention during early diabetes. Pain 2016; 157:910–21
25. Bolyard LA, Van Looy JW, Vasko MR: Sensitization of rat sensory neurons by chronic exposure to forskolin or 'inflammatory cocktail' does not downregulate and requires continuous exposure. Pain 2000; 88:277–85
26. Spahn V, Stein C, Zöllner C: Modulation of transient receptor vanilloid 1 activity by transient receptor potential ankyrin 1. Mol Pharmacol 2014; 85:335–44
27. Al-Madol MA, Shaqura M, John T, Likar R, Ebied RS, Schäfer M, Mousa SA: Comparative expression analyses of pro- *versus* anti-inflammatory mediators within synovium of patients with joint trauma, osteoarthritis,

and rheumatoid arthritis. Mediators Inflamm 2017; 2017:9243736
28. Shaqura M, Khalefa BI, Shakibaei M, Zöllner C, Al-Khrasani M, Fürst S, Schäfer M, Mousa SA: New insights into mechanisms of opioid inhibitory effects on capsaicin-induced TRPV1 activity during painful diabetic neuropathy. Neuropharmacology 2014; 85:142–50
29. Mousa SA, Shaqura M, Al-Madol M, Tafelski S, Khalefa BI, Shakibaei M, Schäfer M: Accessibility of axonal G protein coupled mu-opioid receptors requires conceptual changes of axonal membrane targeting for pain modulation. J Control Release 2017; 268:352–63
30. Gomez-Sanchez E, Gomez-Sanchez CE: The multifaceted mineralocorticoid receptor. Compr Physiol 2014; 4:965–94
31. Manders EM, Verbeek FJ, Aten JA: Measurement of colocalization of objects in dual-color confocal images. J Microsc Oxford 1993; 169:375–82
32. Slight SH, Ganjam VK, Gómez-Sánchez CE, Zhou MY, Weber KT: High affinity NAD(+)-dependent 11 beta-hydroxysteroid dehydrogenase in the human heart. J Mol Cell Cardiol 1996; 28:781–7
33. Chapman K, Holmes M, Seckl J: 11β-hydroxysteroid dehydrogenases: Intracellular gate-keepers of tissue glucocorticoid action. Physiol Rev 2013; 93:1139–206
34. Lijnen P, Petrov V: Induction of cardiac fibrosis by aldosterone. J Mol Cell Cardiol 2000; 32:865–79
35. MacKenzie SM, Clark CJ, Fraser R, Gómez-Sánchez CE, Connell JM, Davies E: Expression of 11beta-hydroxylase and aldosterone synthase genes in the rat brain. J Mol Endocrinol 2000; 24:321–8
36. MacKenzie SM, Lai M, Clark CJ, Fraser R, Gómez-Sánchez CE, Seckl JR, Connell JM, Davies E: 11beta-hydroxylase and aldosterone synthase expression in fetal rat hippocampal neurons. J Mol Endocrinol 2002; 29:319–25
37. Prager EM, Brielmaier J, Bergstrom HC, McGuire J, Johnson LR: Localization of mineralocorticoid receptors at mammalian synapses. PLoS One 2010; 5:e14344
38. Johnson LR, Farb C, Morrison JH, McEwen BS, LeDoux JE: Localization of glucocorticoid receptors at postsynaptic membranes in the lateral amygdala. Neuroscience 2005; 136:289–99

12. List of publications

1. **Doaa Mohamed**, Shaqura, M., Li, X., Shakibaei, M., Beyer, A., Treskatsch, S., Schäfer, M., & Mousa, S. A. (2020). Aldosterone synthase in peripheral sensory neurons contributes to mechanical hypersensitivity during local inflammation in rats. **Anesthesiology**, 132: 867–880. https://doi.org/10.1097/ALN.0000000000003127 **(IF : 7.067)**.

2. Shaqura, Mohammed, Li, L., **Mohamed, D. M**., Li, X., Treskatsch, S., Buhrmann, C., Shakibaei, M., Beyer, A., Mousa, S. A., & Schäfer, M. (2020). Neuronal aldosterone elicits a distinct genomic response in pain signaling molecules contributing to inflammatory pain. **Journal of Neuroinflammation**, 17(1):183 https://doi.org/10.1186/s12974-020-01864-8 **(IF: 5.793).**

3. Tafelski, S., **Mohamed, D**., Shaqura, M., Assaf, C., Beyer, A., Treskatsch, S., Schäfer, M., & Mousa, S. A. (2019). Identification of mineralocorticoid and glucocorticoid receptors on peripheral nociceptors: Translation of experimental findings from animal to human biology. **Brain Research**, 1712(February), 180–187. https://doi.org/10.1016/j.brainres. **(IF: 2.763).**

4. Xiongjuan Li, Mohammed Shaqura, **Doaa Mohamed**, Antje Beyer, Shunji Yamada, Shaaban A. Mousa, Michael Schäfer; (2018), Pro- *versus* Antinociceptive Nongenomic Effects of Neuronal Mineralocorticoid *versus* Glucocorticoid Receptors during Rat Hind Paw Inflammation. **Anesthesiology** ; 28:796–809. https://doi.org/10.1097/ALN. 0000000000002087 **(IF: 6.424).**

5. Aboryag, N. B., **Mohamed, D. M.**, Dehe, L., Shaqura, M., Treskatsch, S., Shakibaei, M., Schäfer, M., & Mousa, S. A. (2017). Histopathological changes in the kidney following congestive heart failure by volume overload in rats. **Oxidative Medicine and Cellular Longevity**, 2017. https://doi.org/10.1155/2017/6894040 **(IF: 4,936).**

6. Shaqura, M., **Mohamed, D. M**., Aboryag, N. B., Bedewi, L., Dehe, L., Treskatsch, S., Shakibaei, M., Schäfer, M., & Mousa, S. A. (2017). Pathological alterations in liver injury following congestive heart failure induced by volume overload in rats. **PloS One**, 12(9). https://doi.org/10.1371/journal.pone.0184161 **(IF: 2.766).**

13. Acknowledgement

I would like to express my gratitude to **Prof. Dr. med. Michael Schäfer** for providing the topic of my PhD thesis and for offering comprehensive care, continuous support throughout the entire PhD period, discussions about experimental settings, scientific questions, and the other issues that evolve during my project for Ph.D. thesis. Additionally, I am also very grateful for his friendly behavior and great help.

I would like to greatly thank **Prof. Dr. Shaaban Mousa** for the co-supervision that made my dissertation possible and for taking on the mentorship. He was always helpful, friendly in answering all questions, and overall was interested in my work in particular in immunohistochemistry. During my years in the Schäfer group, Dr. Mohammed Shaqura helped me with all scientific and technical questions that I had and taught me several helpful operation techniques and behavioral observations. Furthermore, I want to thank all the other laboratory members: Petra von Kwiatkowski, Susana Runewitz, who were always helpful and nice to me and had to endure my special kind of humor particularly at times when I was overexcited or going in the wrong way.

I would like to express my thankfulness to the Egyptian Ministry of Higher Education and Faculty of Science at Aswan University (Aswan, Egypt) for funding the current work. Additionally, I thank all lab members for a great working atmosphere. Thanks, **Drs. Mohammed Al-Madol, Xiongjuan Li and Noureddin Aboryag**. Last, but not least I would like to express my greatest gratitude to my family and friends especially grateful to my parents and my husband for their support, hard patience and endurance during my study. My sons **Yehia**, **Abdalla**, **Adam** and **Wael** thanks a lot for your patience and unlimited love.

Doaa Mohamed